(4)

CHEMICAL
RESEARCH,
DEVELOPMENT &
ENGINEERING
CENTER

CRDEC-TR-200

A METHOD FOR DETERMINING DROPLET SIZE DISTRIBUTIONS AND EVAPORATIONAL LOSSES USING PAPER IMPACTION CARDS AND DYE TRACERS

Douglas R. Sommerville
Joseph E. Matta, Ph.D.

RESEARCH DIRECTORATE

June 1990

U.S. ARMY
ARMAMENT
MUNITIONS
CHEMICAL COMMAND

Aberdeen Proving Ground, Maryland 21010-5423

Disclaimer

The findings in this report are not to be construed as an official Department of the Army position unless so designated by other authorizing documents.

Distribution Statement

Approved for public release; distribution is unlimited.

REPORT DOCUMENTATION PAGE

Form Approved
OMB No. 0704-0188

1. AGENCY USE ONLY (Leave blank)	2. REPORT DATE	3. REPORT TYPE AND DATES COVERED
	1990 June	Final, 88 Mar - 89 Sep

4. TITLE AND SUBTITLE
A Method for Determining Droplet Size Distributions and Evaporational Losses Using Paper Impaction Cards and Dye Tracers

5. FUNDING NUMBERS
PR-1C162622A553I

6. AUTHOR(S)
Sommerville, Douglas R., and Matta, Joseph E., Ph.D.

7. PERFORMING ORGANIZATION NAME(S) AND ADDRESS(ES)
CDR, CRDEC, ATTN: SMCCR-RSP-P, APG, MD 21010-5423

8. PERFORMING ORGANIZATION REPORT NUMBER
CRDEC-TR-200

9. SPONSORING/MONITORING AGENCY NAME(S) AND ADDRESS(ES)

10. SPONSORING/MONITORING AGENCY REPORT NUMBER

11. SUPPLEMENTARY NOTES

12a. DISTRIBUTION/AVAILABILITY STATEMENT
Approved for public release; distribution is unlimited

12b. DISTRIBUTION CODE

13. ABSTRACT (Maximum 200 words)

In liquid spraying operations, droplet size distributions are often measured using paper witness cards. Stain size measurements of collected aerosol stains are converted to the original droplet sizes using a predetermined spreadfactor regression. The regression is developed from control stains. However, drying conditions effecting the spreading process cannot always be matched in the laboratory. Thus, a method of deducing the spreadfactor directly from actual trial stains was developed and tested using thickened diethyl malonate and Whatman #1 Filter Paper. The method uses the spectra properties of the tracer dyes in the test fluid. The dyes are removed by solvent extraction from individual stains on the witness cards and quantitatively analyzed to determine the original droplet size. After the initial study, further work was conducted in measuring droplet free fall evaporation. It was found that the methodology can accurately measure evaporation under field trial conditions.

Keywords:

14. SUBJECT TERMS
~~Witness/impaction~~ cards, Spreadfactors, ~~Droplet free fall~~ evaporation, Dye tracers, Spectroscopy, Droplet size distributions, Falling droplets, Thickened diethyl malonate. (CP)

15. NUMBER OF PAGES
75

16. PRICE CODE

17. SECURITY CLASSIFICATION OF REPORT	18. SECURITY CLASSIFICATION OF THIS PAGE	19. SECURITY CLASSIFICATION OF ABSTRACT	20. LIMITATION OF ABSTRACT
UNCLASSIFIED	UNCLASSIFIED	UNCLASSIFIED	UL

Blank

PREFACE

The work described in this report was authorized under Project No. 1C162622A553I, CB Simulants, Survivability, and Systems Science. This work was started in March 1988 and completed in September 1989. The experimental data are recorded in laboratory notebooks 87-0176, 88-0059, and 89-0072.

The use of trade names or manufacturers' names in this report does not constitute an official endorsement of any commercial products. This report may not be cited for purposes of advertisement.

This report has been approved for release to the public.

Acknowledgments

The authors wish to acknowledge with sincere appreciation the laboratory assistance of Paulette Jones (CRDEC), Angela R. Farenwald (CRDEC), Dorothea A. Paterno (CRDEC), and Jon H. Buschhorn (High School Summer Apprentice), as well as the assistance of Ronald B. Crosier (CRDEC) and Larry M. Sturdivan (CRDEC) in the area of statistical analysis.

Blank

CONTENTS

		page
1.	OBJECTIVE	9
2.	BACKGROUND	9
2.1	General Information on the Spreadfactor Relationship	9
2.2	USDA Forest Service Approach to Spreadfactor Determination	10
2.3	Previous CRDEC Approaches to Spreadfactor Determination	12
3.	PHASE I--EVALUATION OF THE SPECTROSCOPY APPROACH TO SPREADFACTOR DETERMINATION	13
3.1	Introduction	13
3.2	Experimental Method	14
3.2.1	Test Solution	14
3.2.2	Test Procedure	15
3.2.3	Analytical Procedure	16
3.2.4	Experimental Design	17
3.3	Results	18
3.4	Discussion	27
3.4.1	Accuracy of Method	29
3.4.2	Sensitivity of Method	30
3.4.3	Effect of Droplet Impact Velocity on Spreadfactor	31
3.4.4	Advantages and Disadvantages of Method	31
4.	PHASE II--APPLICATION OF METHODOLOGY IN THE EVALUATION OF DROPLET EVAPORATION DURING FREE FALL	32
4.1	Introduction	32
4.2	Experimental Method	33
4.2.1	Test Solution	33
4.2.2	Test Procedure	34
4.3	Results	34
4.3.1	Experimental Data and Analysis	34
4.3.2	Error Analysis	38
4.4	Discussion	40
5.	CONCLUSIONS	40
6.	RECOMMENDATIONS	41
6.1	Accuracy of Methodology and Dye Photostability	41
6.2	Calibration Stains	42
	LITERATURE CITED	43

APPENDIXES

A. INSTRUMENT DESCRIPTION/OPERATING PARAMETERS AND DYE CHARACTERISTICS 45

B. USE OF A MULTIPLE CORRELATION/REGRESSION FOR A THREE VARIABLE SYSTEM 49

C. USE OF MONTE CARLO SIMULATION FOR ERROR ANALYSIS OF PHASE II RESULTS 59

D. EXPERIMENTAL DATA AND REGRESSION ANALYSIS RESULTS FOR PHASE I RESULTS 69

E. EXPERIMENTAL DATA AND REGRESSION ANALYSIS RESULTS FOR PHASE II RESULTS 73

LIST OF FIGURES

1. Drop vs. Stain Diameter Regression--Set A (1 day) 19

2. Drop vs. Stain Diameter Regression--Set B (3 days) 20

3. Drop vs. Stain Diameter Regression--Set C (1 week) 21

4. Drop vs. Stain Diameter Regression--Set D (2 weeks) 22

5. Drop vs. Stain Diameter Regression--Set E (4 weeks) 23

6. Spreadfactor Comparison--WDT & Spray Booth Stains 24

7. UV/VIS vs. Fluorescence Spectroscopy Analysis ... 26

8. Comparison of Spectroscopy vs. Mass Balance 28

9. Initial Droplet Diameter vs. Stain Diameter Test Conducted Using DEM and Blotter Witness Cards 35

10. Reference Spreadfactor Curves as Function of R_c for Stains Made with DEM on Blotter Paper 36

LIST OF TABLES

1. WDT Droplets D_d--Mass Balance vs. Spectroscopy .. 29

2. Comparison of Measured and Predicted R_c Values .. 38

3. Monte Carlo Simulation Error Estimates from R_c Obtained from Eq. (3) 39

DIAGRAM

Droplet Free Fall/Witness Cards 11

Blank

A METHOD FOR DETERMINING DROPLET SIZE DISTRIBUTIONS AND EVAPORATIONAL LOSSES USING PAPER IMPACTION CARDS AND DYE TRACERS

1. *OBJECTIVE*

Paper witness cards are commonly used to measure and evaluate the size distributions of aerosol spray droplets in open air dissemination trials. The impacted drops are allowed to dry, and the resultant size distribution of the spot signatures (which is commonly enhanced through the use of tracer dyes) is measured. However, to determine the airborne drop size distribution, one must establish a spreadfactor relationship which converts the measured stain size to the original drop size. This relationship can be determined from controlled laboratory tests and/or actual trial data.

The objective of the present work is to evaluate the novel use of ultraviolet/visible and fluorescent spectroscopy to directly deduce the spreadfactor relationships for drops sampled on witness cards, as well as to explore the application of this method towards evaluating individual droplet free fall evaporational losses. Potential problems with dye degradation and their effects on the methodology's accuracy are also examined in the present work. In addition, the effectiveness of a specific simulant/tracer dye/witness card combination currently under consideration for a field trial program was evaluated for use with this methodology.

2. *BACKGROUND*

2.1 *General Information on the Spreadfactor Relationship*

The spread factor relationship is known to be dependent upon the physical properties of the fluid, drying conditions, (e.g. temperature/humidity and wind speed) and the type of paper employed. The impact velocity of the droplet on the witness card can also influence the spread factor relationship in some instances, depending on the type of paper used and the physical properties of the fluid.[1,2]

The spread factor relationship has been expressed mathematically in many different forms: linear, polynomial, and power law. The first two forms have been found to be suitable for water and oil based insecticidal formulations,[1] but for polymer thickened (viscoelastic) solutions, a power law curve of drop diameter (D_d) versus the stain diameter (D_s) has been found to best correlate the spreadfactor data (over a droplet diameter range of 2 to 3 logarithmic cycles), i.e.[3]:

$$(1) \qquad D_d = aD_s^b$$

where "a" and "b" are constants dependent on the specific test fluid, ambient experimental conditions, and type of sample paper used (see Diagram 1 for definition of terms).

There are two primary sources of error involved in the use of Eq. (1): the experimental determination of the constants a and b; and the actual measurement of D_s. The objective of the present work is to develop a more accurate means of determining the former.

The latter is no less important, and the accuracy in measuring D_s is greatly influenced by the tracer dye/witness card/test fluid combination used. A poor choice of tracer dye/witness card for a test fluid could result in a poorly defined stain boundary, making it difficult to accurately measure D_s. Usually, testing is conducted (simply by generating stains and observe the resulting stain contrast) to arrive at a suitable tracer dye/witness for the fluid of interest prior to work on determining a and b. The evaluation of the numerous tracer dyes/witness cards/test fluid combinations possible is beyond the scope of the present work. However, this issue has been addressed for insecticidal sprays.[1]

2.2 *USDA Forest Service Approach to Spreadfactor Determination*

The USDA Forest Service has done extensive work on perfecting the use of witness cards/spreadfactors, particularly in the sampling of insecticidal sprays used in forest and crop protection. The exact employment of paper witness cards for this purpose has been extensively reviewed by one of their technical publications.[1]

The basic approach employed by the USDA Forest Service in determining spreadfactors is to used a vibrating reed apparatus (similar to that described by

DROPLET FREE FALL/WITNESS CARDS

DEFINITION OF TERMS

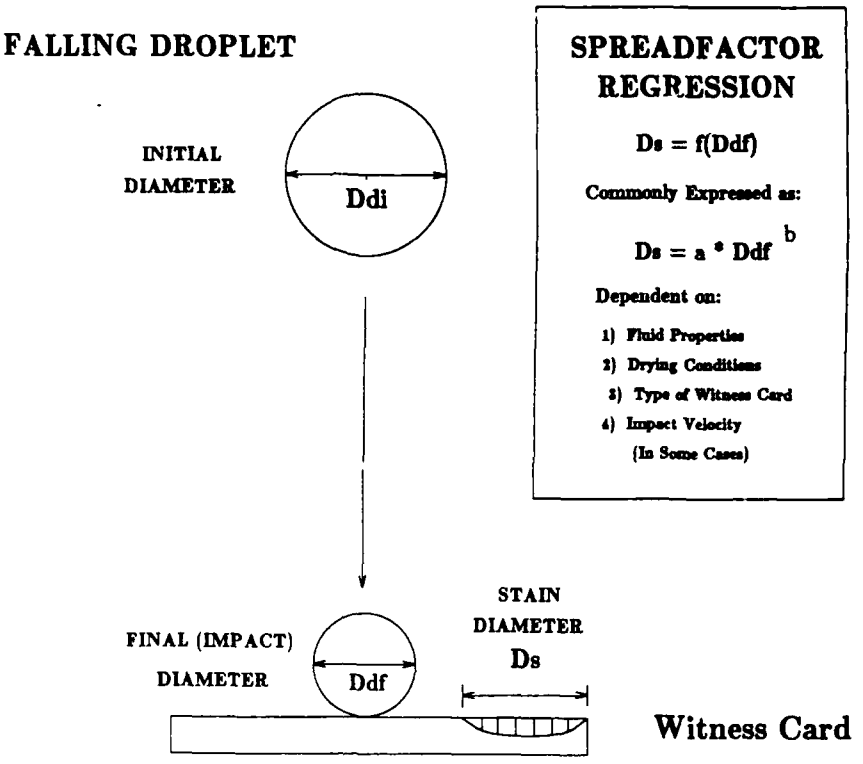

DIAGRAM

Davis (1951)[4] and Maksymiuk and Moore (1962)[5]) to generate droplets of uniform size (from 50 to 500 μm in diameter) under laboratory conditions.[1] The exact size of the droplets generated were measured by catching the droplets on magnesium oxide (MgO) coated slides and measuring the depth of the resulting crater and using the necessary conversion factor as described by May (1950)[6] to translate the crater depth to a corresponding droplet diameter. After finding D_d for a particular setting of the apparatus using the MgO-coated slides, witness cards would then be substituted for the slides. The droplets impacting on the cards would then be allowed to dry, after which D_s would be measured. A tracer dye is commonly added to the test fluid for stain enhancement.

The advantage of the USDA Forest Service approach is that spreadfactors can be accurately determined for very small droplet sizes with a high degree of reproducibility under laboratory conditions. However, the validity of the application of laboratory-derived spreadfactors to stains generated in an outdoor field trial is questionable. Many variables influence the spreadfactor, and the exact matching of drying conditions under laboratory conditions with that experienced in a field trial is difficult. Thus, it is highly desirable to use the actual aerosol as generated in a field trial to directly determine the spreadfactor.

2.3 *Previous CRDEC Approaches to Spreadfactor Determination*

Previously, CRDEC has determined the spreadfactor relationship through the formation and individual measurement of single droplets in the laboratory environment, but in a somewhat different manner than the USDA Forest Service. Polymer thickened (viscoelastic) solutions of interest to CRDEC cannot be effectively broken into suitable size droplets using the vibrating reed apparatus due to the viscoelasticity of the solutions involved. Instead, to generate droplets, either an atomizing sprayer or the wire droplet technique (WDT) was used. The latter method consists of dipping a thin wire into a sample of test fluid, so that upon withdrawal the fluid adhering to the wire will eventually form a drop at the wire tip. The drop is then transferred to the desired surface.

Whatever the method of generation, the original droplet diameter was calculated from the droplet's mass and density, with an analytical mass balance being used for the former. MgO-coated slides were not used by CRDEC for droplet sizing since this method is better suited for calibrating a stream of similar sized droplets (ie. from a vibrating reed apparatus) as opposed to the random drop generation of a hand sprayer.

The dependence on measuring the droplet's mass is a major limitation since droplet diameters smaller than 800 microns are difficult to individually generate and weigh with an acceptable degree of confidence. This is a severe limitation since many droplets produced during dispersion trials may be smaller than 800 microns. Consequently, the spread factor relationship is frequently applied to stain sizes outside of the droplet range from which it was deduced.

Besides the difficulty in obtaining accurate droplet mass values, there still is a question (as mentioned previously in Section 2.1) on how valid is the application of laboratory-derived spreadfactors to stains generated in an outdoor field trial. The solution to this problem as shown in the present work is to use the actual field trial data for spreadfactor derivation.

3. *PHASE I--EVALUATION OF THE SPECTROSCOPY APPROACH TO SPREADFACTOR DETERMINATION*

3.1 *Introduction*

Instead of directly measuring the mass of individual droplets (and then using the fluid density) to obtain D_d, the current study used the ultraviolet/visible and fluorescent spectra properties of tracer dyes that were previously added in known quantities to the test liquid. Using solvent extraction, the tracer dyes were removed from individual droplet stains on the witness cards and quantitatively analyzed. By determining the amount of dye present, the original droplet size is then calculated using the known weight fraction of the dye in the original test solution.

The use of the spectra properties of the tracer dye is a good idea in principle. However, liquid dissemination trials are often conducted under sunny skies, providing the opportunity for solar degradation of the dye. Also, delay between the collection of the stains and their subsequent analysis usually occurs in large-scale testing, which may allow the dye to degrade and set into the paper. Because of the possible adverse effects of solar exposure and aging, further investigation is required before the method can be used extensively.

3.2 *Experimental Method*

3.2.1 *Test Solution*

A polymer-thickened solution of diethylmalonate (DEM), prepared using an 3.5 g/dl concentration of Rohm and Haas K-125 (a copolymer of 80% polymethyl methacrylate and 20% poly (ethyl/butyl) acrylate), was employed for this phase of the present work. A DEM/K-125 solution was chosen due to its frequent use as a simulant in dissemination studies. The density of pure DEM and thickened DEM (for the polymer concentrations of interest) have been found to be of the same density (1.055 g/ml) in various unpublished CRDEC sources.

Two tracer dyes were added to this solution: Tinopal SWN Dye (also known commercially as Calcofluor White RW or RWP Concentrate) and Ceres Blue ZV (also known commercially as Calco Oil Blue ZV) Dye. A more complete description of these dyes is presented in Appendix A.

Tinopal SWN Dye is a fluorescence dye which has been used as a whitening agent commerically for paper and cloth. It has a substantial absorbance peak in the ultraviolet region of the spectrum, and this peak was employed in the present study for analytical purposes. Ceres Blue ZV Dye has been commonly used for enhancing stain contrast on witness cards in previous dissemination studies conducted by CRDEC. Even though the primary purpose of Ceres Blue ZV is stain enhancement, the dye also could be, and was, used in the quantitative measurement of drop mass through the spectroanalysis of the visible light region.

Nominally, 1.0 wt % of Tinopal and 2.0 wt % Ceres Blue were added to the DEM/K-125 solution. The exact amounts of each in the test solution were determined through ultraviolet/visible absorbance measurements. This knowledge was subsequently used to convert measured fluorescence/absorbance measurements of test solutions to corresponding droplet mass/diameter values. To prevent possible dye degradation, the prepared DEM/K-125 solutions were kept in opaque containers and in a dark location when not being used.

3.2.2 *Test Procedure*

Droplets of the DEM/K-125 solution were generated using a spray booth 4 x 4 feet at the base and 20 feet tall. Inside the booth, a Spraying Systems Air Atomizating Nozzle Set-up #E15B was mounted at 18 feet in the center of the booth. The DEM/K-125 solution was placed in a holding reservoir and then was extruded vertically downward through the nozzle using approximately 2 psi of pressure. Inside the nozzle, a second air stream with a pressure of 8 psi was used to aerosolize the solution as it exited the nozzle. Due to the initial downward velocity imparted by the spraying operation and the distance traveled prior to impact, the generated droplets (for the D_d values of interest–250 to 2500 μm) are essentially travelling at their terminal velocity prior to impact (as determined using the appropriate equations of droplet motion).

Two devices were used to collect the falling drops: an 6 3/4 x 8 3/4 inch metal plate with grooves to hold a slightly smaller witness card; and a rotational sampling device, which was used previously in other field studies.[3] The rotational sampling device consisted of a circular (30.5 cm diameter) paper sheet rotating (10 rpm) under a cover having a sector shape (58 sq. cm.) opening. As the drops settie towards the ground a new portion of the sampling sheet is continously exposed. This decreases the density of droplet deposition and loss of data due to overlap that would occur were the drops allowed to cumulatively impact on a stationary sampling area. Whatman No. 1 Filter Paper, which has been used previously for droplet collection, was used for the witness cards. Upon the completion of the spraying, the impacted cards were taken out of the booth and allowed to dry indoors. The cards were kept in a dark location in order to avoid possible dye degradation due to light exposure.

Upon drying, the stains were sized on a Quantimet 920 Image Analyzer, manufactured by Cambridge Instruments, Ltd, Cambridge, United Kingdom. With the lens/camera configuration used, the error in D_s was estimated to be $\pm$ 35 μm under ideal conditions. However, under normal experimental conditions (involving less than perfectly defined stain boundaries), the error in D_s is typically double that of the stated error encountered under ideal conditions. The current witness card/tracer dye combination was primarily chosen for use with diethyl malonate because of the well defined stain boundaries achieved, thus improving the accuracy in measuring D_s.

For comparison purposes, droplets were also generated using the WDT, with the drop being transferred to a pre-weighted witness card and the card then re-weighted to determine the drop's mass. These stains were then analyzed in the same manner as those made in the spray booth in order to see if spectroanalysis will produce a drop mass value in agreement with the direct measurement value obtained from an analytical balance. Since the stains formed in the spray booth and by the WDT were allowed to dry under similar ambient air conditions, possible deviations in the spread factor relationships obtained from both WDT and spray booth generated droplets due to differing humidity and temperature conditions were minimized.

3.2.3 *Analytical Procedure*

To determine the amount of dye present in the individual droplet stains, stains were cut out of the witness cards and individually placed in a 10 ml volumetric flask. The flask was then filled to the mark with high purity acetone (with a fluorescence background of less than 1 ppb as quinine sulfate) and placed in a ultrasonic bath for 15 minutes to promote the extraction of the dye from the card. K-125 polymer is soluble in acetone, thus the possibility of the dye not totally diffusing out of the polymer was eliminated.

Stains created with the WDT were used to determined the efficiency in recovering the dye from the card. The appearance of either dye degradation and/or the permanent setting of the dye in the card can effect the efficiency of dye recovery. These two phenomena are primarily dependent on the stain's age, previous solar exposure, and the type of witness card used. Under ideal conditions (ie. solvent extraction performed 24 hours after stain has dried with no solar exposure), the present study confirmed the results of previous unpublished work that at least 99 wt% of the dye was removed from the witness card.

Upon removal from the bath, the acetone solutions were then spectroanalyzed using 3 ml quantities. Solutions that gave off too much fluorescence intensity were further diluted to obtain a fluorescence intensity within the calibration range of the spectrophotometer.

A Perkin Elmer Model LS-3B Fluorescence Spectrophotometer was used to measure the fluorescence of Tinopal SWN Dye, and a Perkin Elmer Lambda 9 UV/VIS/NIR Spectrophotometer was used to measure the absorbance of both

Tinopal SWN and Ceres Blue ZV Dyes. Prior to analyzing the dye stains, calibration curves were made for acetone/dye solutions using prepared solutions of known composition (see Appendix A for the exact procedure employed). The peak absorbance and fluorescence wavelengths used, as well as other pertinent instrument parameters, are listed in Appendix A. Possible background fluorescence interference due to residue from the witness card was also tested for, and it was found to be negligable for the range of Tinopal SWN Dye concentrations employed in the present work.

A dual approach, using fluorescence and absorbance measurements, was used due to the complementary qualities of the two methods. Fluorescence spectroscopy is very sensitive, capable of detecting fluorescent dye concentrations on the order of 1 ng/ml, but erroneous results can easily occur due to the presence of very low levels of contaminants introduced in the normal course of laboratory work. Ultraviolet/visible spectroscopy is not as sensitive as fluorescence, only being able to detect minimum dye concentrations on the order of 1 ug/ml (a factor of 1000 difference compared to fluorescence spectroscopy), but it is less susceptible to background interference from contamination. Thus, using both methods of analysis provides a ready verification of the accuracy of results obtained by either. However, for the low dye concentrations (i.e. less than 0.5 ug/ml) UV/visible spectroscopy was not sufficiently sensitive and thus only fluorescent measurements were obtained.

3.2.4 *Experimental Design*

A total of 80 stains generated in the spray booth were used in the present work, with diameters ranging from 600 to 7200 microns, and were randomly divided into five sets of 16 stains each. One set of stains was extracted and analyzed 1 day, 3 days, 1 week, 2 weeks, and 4 weeks after being created. This was done in order to determine if any dye degradation occurred even when the stains were stored in the dark.

On the same day that these stains were created, 15 stains were maded using the WDT. Their drop masses were determined gravimetrically on a Mettler AE160 Electronic Balance with an accuracy of $\pm$ 0.02 mg. To reduce the possible effects of systematic error that may have occurred while making the stains, the stains were randomly divided among the 5 sets of spray booth stains, 3 to a set. The WDT stains were made to serve as a check on the accuracy of the analytical procedure.

As mentioned previously, the spread factor relationship may be influenced by the impact velocity of the droplet. In order to determine whether this was the case with the simulant/witness card combination being used in the present study, the WDT stains (negligible impact velocity) were compared with spray booth stains (terminal velocity upon impact) to see if any difference existed in the spreadfactor relationship.

3.3 *Results*

Stain diameters ranging from 600 to 13,000 microns (which roughly corresponds to drop diameters of 250 to 2300 microns) were analyzed (see Appendix D for a listing of the experimental data). For drop diameters lower than approximately 700 to 800 microns and for the particular weight percent of the dyes present in the simulant, only fluorescence spectroscopy could be use to quantitatively analyze the amount of dye (Tinopal SWN) present in individual stains. Thus for continuity, only fluorescence data was used to determine the spread factor relations over the entire range of interest, with the absorbance data being used to verify the accuracy of the former.

Figures 1-5 present the individual results of Sets A-E in terms of drop diameters obtained from fluorescence spectroanalysis and stain diameters measured with the Quantimet 920. Also shown for comparison is the data obtained from the WDT technique. A least squares regression analysis was performed based on a log-log plot of each of the individual sets (Sets A-E), and the result (solid line), along with the 95% confidence level boundaries as determined from the results of the regression analysis (dashed lines), are shown in the figures (see also Appendix D for regression results). No statistically significant differences were found upon the comparison of the five data sets. This indicates that there was no dye loss for up to 4 weeks after the stains were made for samples not exposed to light.

Since there is no significant difference among the data sets of spray booth stains, a linear regression analysis was then performed by combining all the data sets together. The resulting line equation, as well as the data points from all five sets, with 95% confidence levels is shown in Figure 6. Based on the linear regression analysis of the five data sets, the random error involved in a subsequent estimate of $\log_{10} D_d$ based upon a measured value of $\log_{10} D_s$ is $\pm$ 0.034 (95% confidence). On a linear basis, for $D_d = 1000\ \mu$m, this is approximately an 8% error.

FIGURE 1

Drop vs. Stain Diameter Regression--Set A (1 day)

From Fluorescence Analysis of Spray Booth Data

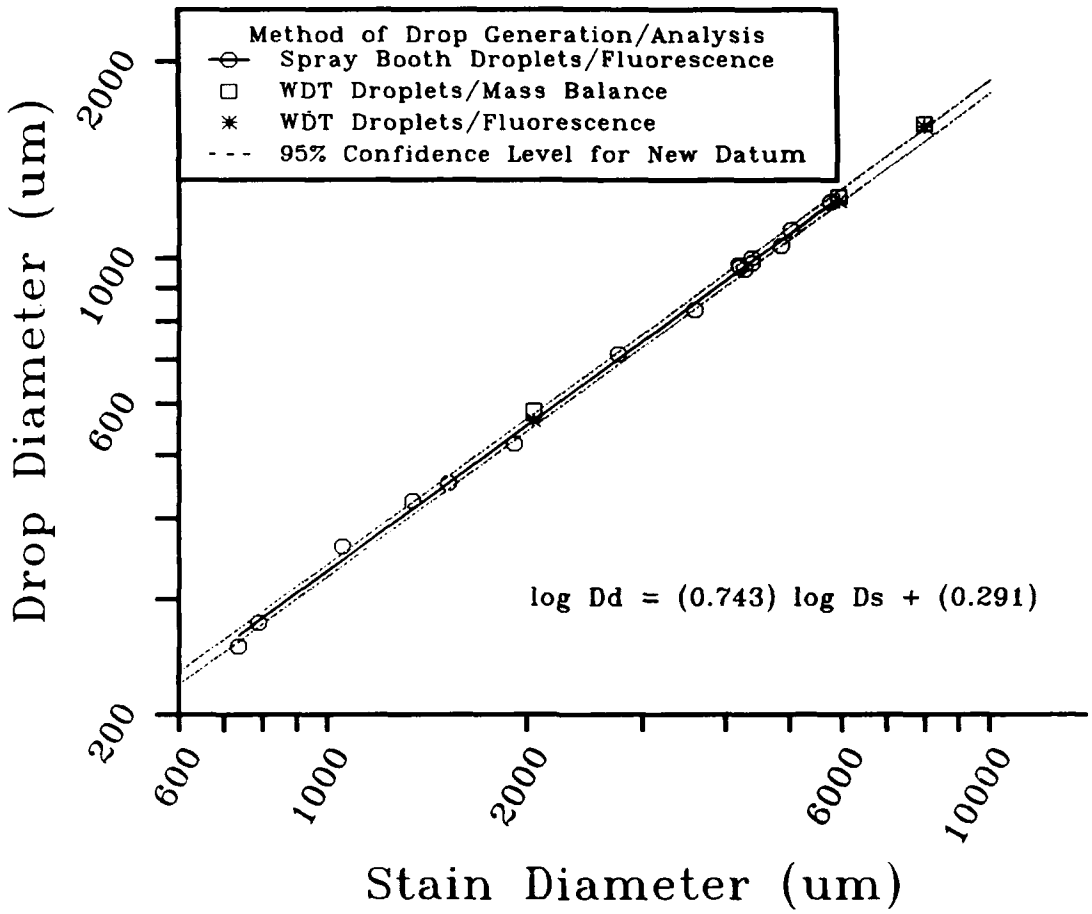

FIGURE 2

Drop vs. Stain Diameter Regression--Set B (3 days)

From Fluorescence Analysis of Spray Booth Data

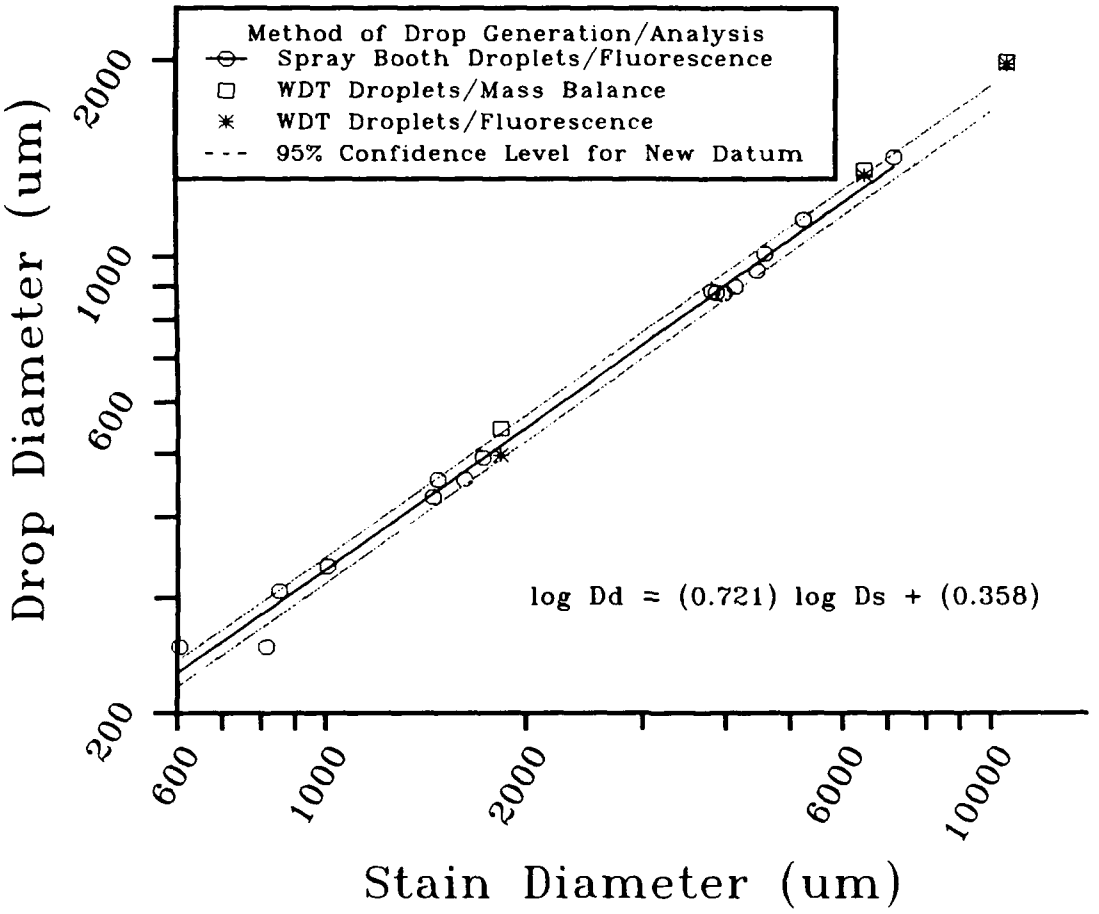

FIGURE 3

Drop vs. Stain Diameter Regression--Set C (1 week)

From Fluorescence Analysis of Spray Booth Data

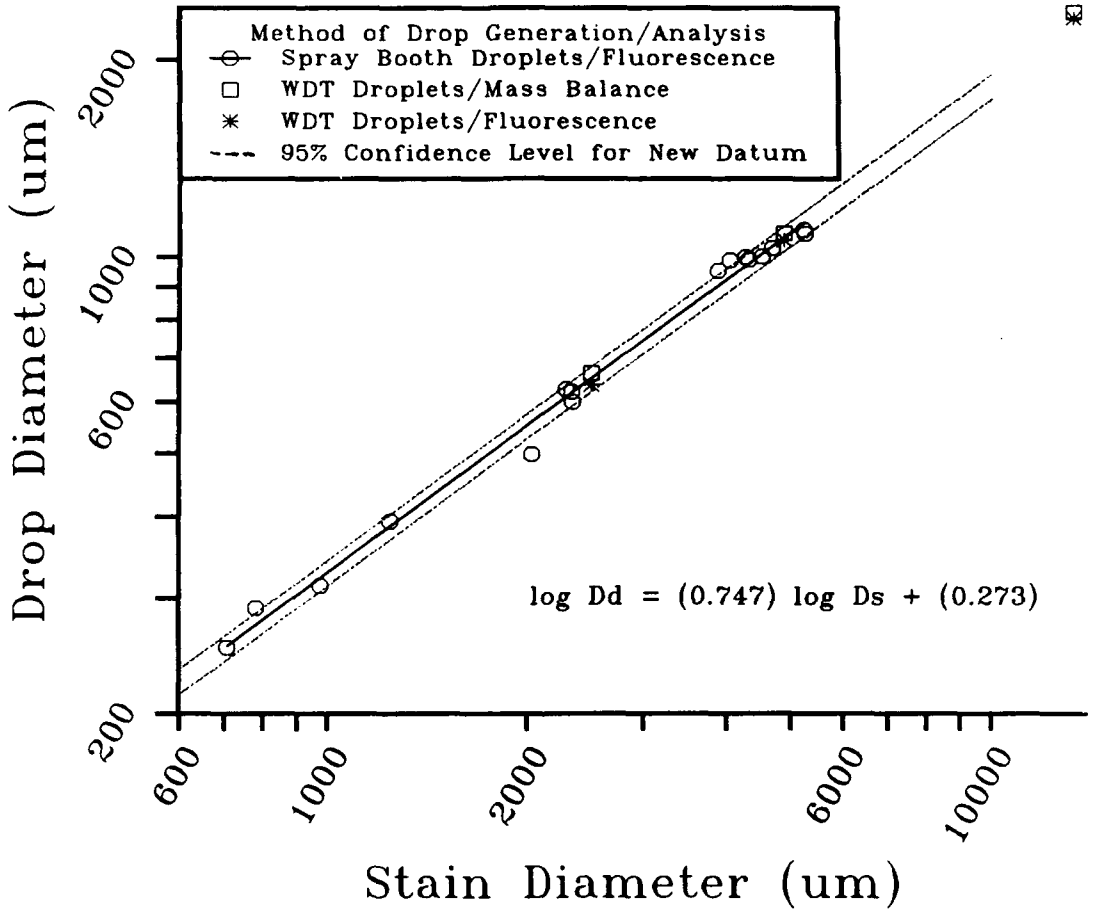

FIGURE 4

Drop vs. Stain Diameter Regression–Set D (2 weeks)

From Fluorescence Analysis of Spray Booth Data

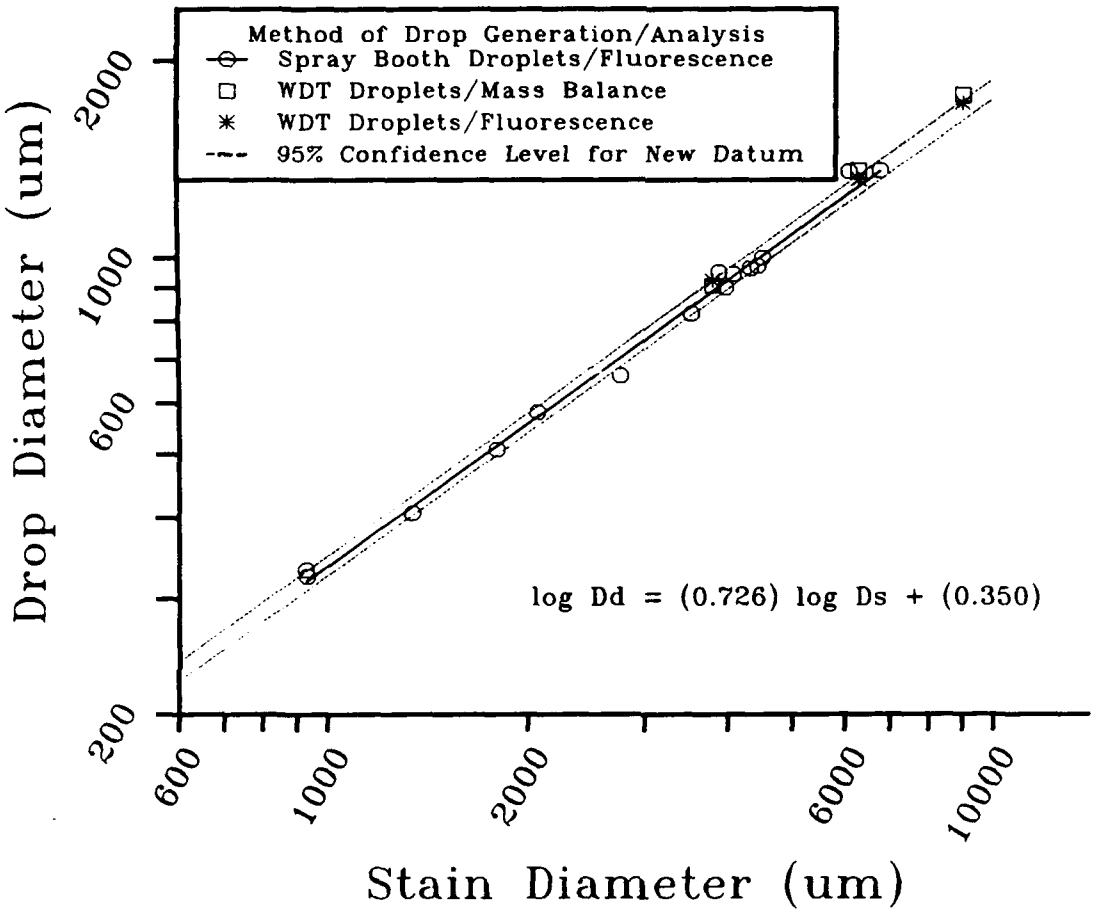

FIGURE 5

Drop vs. Stain Diameter Regression–Set E (4 weeks)

From Fluorescence Analysis of Spray Booth Data

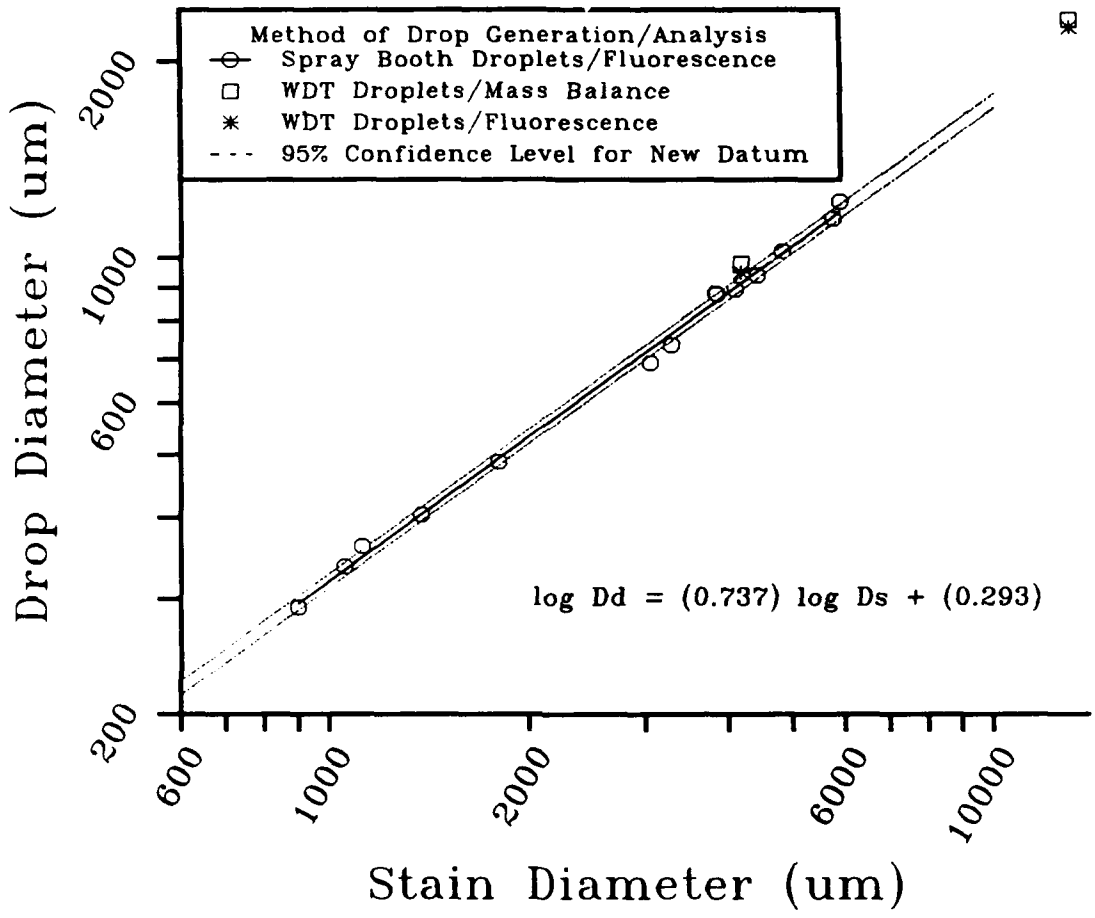

FIGURE 6

Spreadfactor Comparison--WDT & Spray Booth Stains

From Direct Measurement and Fluorescence Analysis

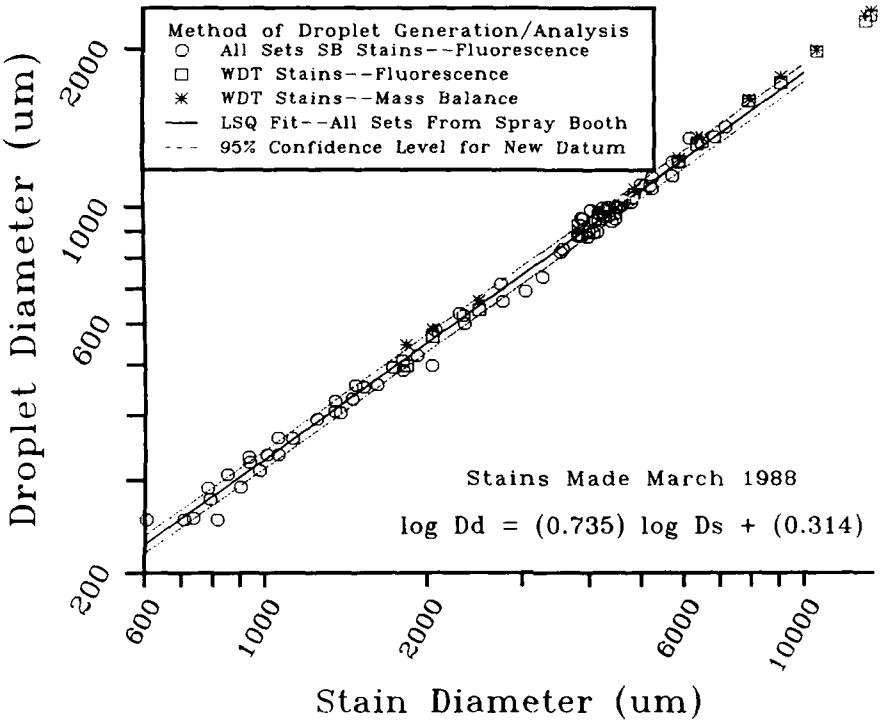

Also included in Figure 6 for comparison are D_d and D_s values for WDT droplets obtained from fluorescence analysis. As seen in Figure 6, there is no statistically significant difference between the spread factors obtained for zero velocity drops (WDT) and those droplets traveling at approximately their terminal velocity (Spray Booth).

In Figure 7, a comparison is presented between drop diameter values obtained by measuring absorbance, $D_{d_{abs}}$, versus that by measuring fluorescence, $D_{d_{fluor}}$, for the spray booth droplets. $D_{d_{fluor}}$ versus D_s data is presented in form of the line equation as originally shown in Figure 6. The actual $D_{d_{abs}}$ versus D_s data points are plotted individually, and they are broken down into three groups based upon the wavelength, λ, (in nm) used: $D_{d_{\lambda=366}}$, $D_{d_{\lambda=508}}$, and $D_{d_{\lambda=645}}$. The first λ corresponds to the absorbance peak for Tinopal SWN Dye and the latter two are absorbance peaks of Ceres Blue ZV Dye.

Though in general all of the data is centered around the line equation, $D_{d_{\lambda=366}}$ values are slightly higher than the $D_{d_{\lambda=508}}$ and $D_{d_{\lambda=645}}$ values for a given D_s value. Also, $D_{d_{\lambda=366}}$ values tend to be higher than $D_{d_{fluor}}$, while $D_{d_{\lambda=508}}$ and $D_{d_{\lambda=645}}$ tend to be lower than $D_{d_{fluor}}$.

The difference between $D_{d_{\lambda=508}}$ and $D_{d_{\lambda=645}}$ values in comparison to $D_{d_{fluor}}$ and $D_{d_{\lambda=366}}$ could be due to varying rates of dye aging between Ceres Blue ZV Dye and Tinopal SWN Dye, with the former suffering at a greater rate. Subsequent studies (to be published in a future work) have observed such a phenomena.

The slight difference between $D_{d_{\lambda=366}}$ and $D_{d_{fluor}}$ values, being based upon the different spectral properties of Tinopal SWN Dye, cannot be attributed to dye aging. There are two probable reasons for this difference. First, separate calibration curves had to be prepared for interpreting each spectra property (fluoresence and absorbance) of Tinopal SWN Dye as a function of its concentration in an acetone solution. Ideally, the calibration curves should produce the same dye concentration value given a particular set of fluoresence intensity and absorbance values from a sample solution. However, in practice, such agreement is rare. In this instance, the disagreement is primarily due to the differing measurement sensitivities of the analytical instruments used (LS-3B [for fluorescence] and Lambda 9 [for absorbance] spectrophotometers) and the experimental error involved in the preparing the curves.

FIGURE 7

UV/VIS vs. Fluorescence Spectroscopy Analysis

Analysis of Spray Booth Stains

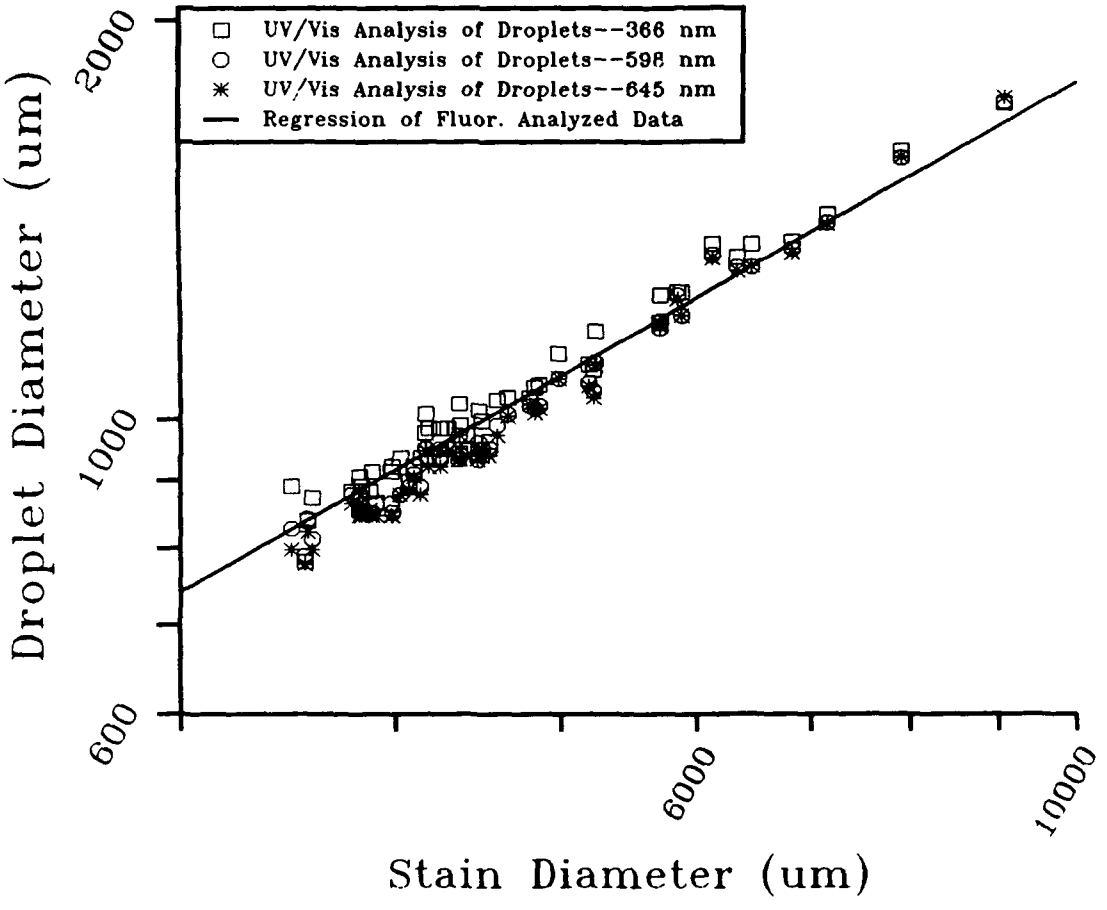

Second, the measurement of fluorescence usually involves the additional dilution of the original sample solution (see Section 3.2.3) prior to analysis. This introduces a potential source of experimental error not found with the absorbance measurements. Errors associated with dilution are of two types: inaccurate volume measurements in the making of the actual dilution, or the introduction of additional background fluorescence through the use of improperly cleaned glassware. It should be noted that any acetone solution having an appreciable absorbance (under the conditions of the present study) will have to be diluted prior to measuring fluorescence, which was the situation for the vast majority of the data presented in Figure 7.

The accuracy of the spectroscopically derived spreadfactor can best be gauged by examining the results obtained from the WDT droplets, shown in Table 1. The results of both the fluorescence and absorbance analysis, as well the original mass balance measurements, for the WDT droplets among the five data sets are presented in terms of D_d in the table. In Figure 8, the results are graphically depicted, with values from both fluorescence and absorbance, $D_{d_{spec}}$, being plotted against the corresponding value obtained from the direct mass balance measurement, $D_{d_{mass}}$. For convenience, lines representing 0% (slope of the line equaling 1) and 5% difference (slope of the lines being 1.05 and 0.95) between the $D_{d_{spec}}$ and $D_{d_{mass}}$ values are also shown in the figure.

The vast majority of points lay within the region between the two 5% difference lines, signifying that the $D_{d_{spec}}$ values are in agreement within 5% of the $D_{d_{mass}}$ values. However, there is a slight tendency for $D_{d_{mass}}$ to be greater than the corresponding $D_{d_{spec}}$ values. The slight tendency may be due to a small amount of dye degradation due to aging and setting into the witness card paper on the part of Tinopal SWN Dye. The "shelf life" of Tinopal SWN Dye (the point in time after the sample is made where dye degradation causes a significant deviation {approximately 2 to 5%} between $D_{d_{spec}}$ and $D_{d_{mass}}$) is beyond the scope of the present work.

3.4 *Discussion*

Based on Phase I results, the use of fluorescence and UV/VIS spectroscopy has excellent potential for determining droplet spread factors. The resulting linear regression analysis using a power law relation of the D_d versus D_s data for a

FIGURE 8

Comparison of Spectroscopy vs. Mass Balance

Droplet Diameter Values from WDT Stains--All Sets

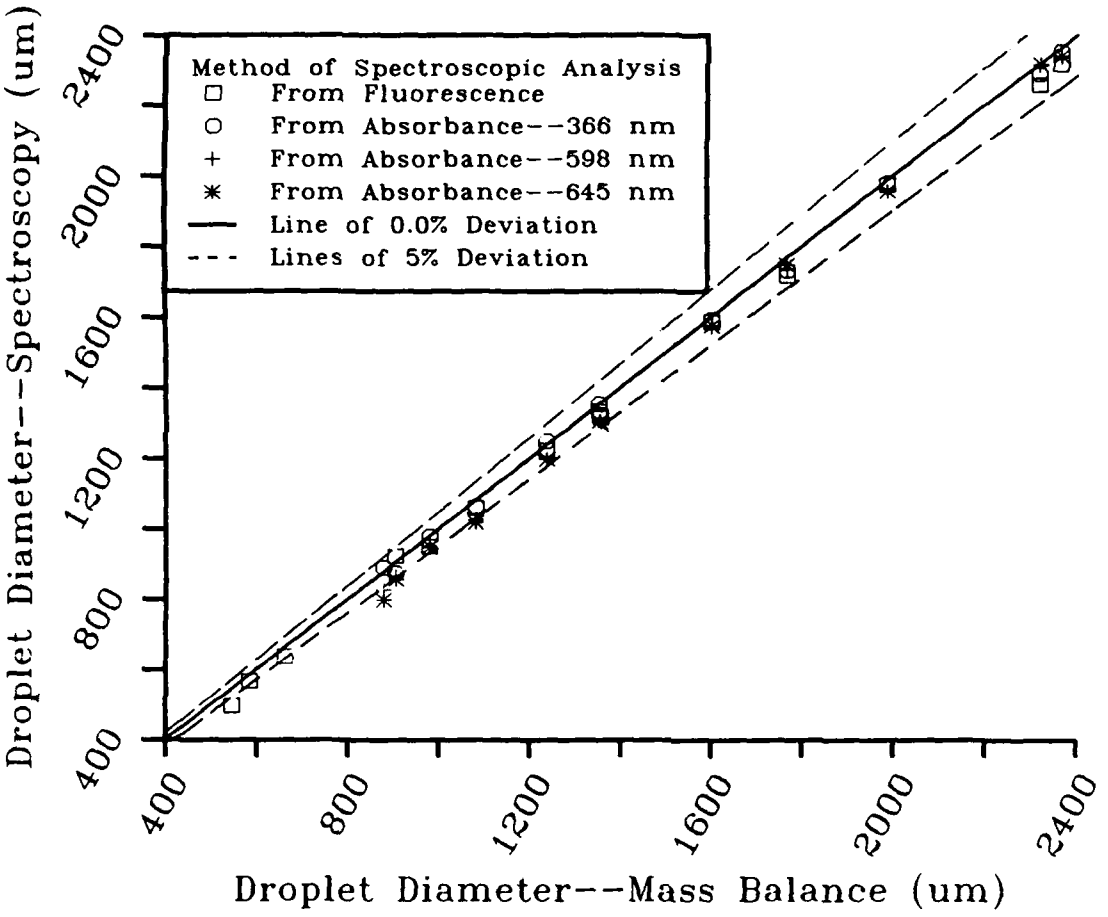

TABLE 1

WDT Droplets D_d--Mass Balance vs. Spectroscopy

Set	D_d μm Based Upon Measurements From					D_s μm
	Fluor.	Absorbance at λ {nm} 366	598	645	Mass Blnc.	
A	565				584	2050
	1223	1248	1198	1198	1239	5890
	1587	1592	1572	1576	1602	7920
B	497				546	1833
	1332	1353	1302	1304	1354	6479
	1974	1980	1956	1956	1988	10565
C	636				662	2505
	1059	1062	1024	1018	1082	4859
	2319	2355	2338	2341	2366	13270
D	922	873	864	855	905	3825
	1316	1324	1302	1294	1357	6352
	1717	1730	1733	1747	1767	9087
E		890	827	797	879	3483
	949	977	950	947	980	4166
	2259	2289	2315	2319	2320	12989

viscoelastic DEM solution show comparatively little experimental scatter (see Figure 6).

3.4.1 *Accuracy of Method*

The accuracy of the method was found to be excellent, with droplet mass values obtained by the present method agreeing favorably with directly measured values using a mass balance (see Figure 8). However, this accuracy is highly dependent on the photostability of the tracer dyes employed, with care having to be exercised to avoid loss in accuracy due to dye aging or setting.

The photostability of Tinopal SWN Dye (the primary tracer dye) was not found to be a problem in the present study. The $D_{d_{fluor}}$ values for Set E (analyzed four weeks after creation) showed no visible (statistically significant) effect when compared with other samples analyzed at earlier dates (Sets A-D). However, some slight deviation (less than 5%) between $D_{d_{spec}}$ and $D_{d_{mass}}$ values for the WDT droplets is evident in Figure 8. As mentioned in Section 3.3, further work should be done to establish the "shelf life" of Tinopal SWN Dye.

Photostability of the dye is a particular concern because fluorescent dyes like Tinopal SWN are generally more vunerable than other dyes to solar degradation. In the present work, the stains were not exposed to sunlight in order to prevent possible solar degradation effects from interferring with the evaluation of the spread factor analysis technique and dye degradation due to aging. However, in actual field trials, solar degradation could be a factor that must be considered, especially if witness cards are left out in the sun for long periods of time before collection. Preliminary (unpublished) work performed by the authors prior to the present study has found this to be a factor in some cases. The in-depth testing required to quantitatively determine the photostability of the dyes of interest is beyond the scope of the present work.

3.4.2 *Sensitivity of Method*

Droplet diameters as low as 250 microns can be accurately measured using solvent extraction of the stains from the witness cards and fluorescence spectroscopy to analyze the resulting solution. UV/VIS spectroscopy can also be used, but it does not have the sensitivity to accurately measure droplets (made from solutions nominally having 1-2 wt.% of a tracer dye) below 600 to 700 microns. However, since UV/VIS spectroscopy is not as prone as fluorescence spectroscopy to errors resulting from impure solvents, UV/VIS spectroscopy is useful in verifying the results of fluorescence spectroscopy, at least for droplets greater than 700 microns.

The exact sensitivity and experimental limits of the spectroscopy approach is dependent on the properties and amount of the dye used. However, some general estimates can be made for most dyes. Commonly, tracer dyes are not used in quantities exceeding 2 to 3 weight % of the total test solution so that the physical properties of the fluid will remain essentially unchanged. If two droplets, with diameters of 1000 and 100 microns, were made from a 2 weight % dye

solution, the mass of dye available for analysis from each droplet are approximately 10 and 0.01 ug, respectively. If 10 ml of solvent (such as acetone or isopropanol) is used for extracting the stain from the paper, dye concentrations of 1 to 0.001 ug/ml are obtained. Ultraviolet/visible absorbance measurement are accurate down to approximately 1 to 0.5 ug/ml, while fluorescence measurements can be used accurately for dye concentrations as low as 0.01 to 0.001 ug/ml. Thus, the minimum detectable droplet diameters are 1000 and 100 microns for fluorescence and ultraviolet/visible spectroscopy, respectively. These limits cannot be significantly improved upon without the addition of excessive amounts of dye, since the minimum detectable droplet diameter value is a cubic function of the amount of dye present in the simulant. A thousand fold increase in dye mass would only produce a 10 fold decrease of the minimum detection limit of droplet diameter.

3.4.3 *Effect of Droplet Impact Velocity on Spreadfactor*

The good agreement between spread factor values for drops generated by the WDT and the spray booth implies that static rather than dynamic droplet spreading is the predominant mechanism controlling D_s. This is probably a result of the strong absorption and wicking potential of Whatman #1 paper. However, should less absorbent paper be used, the droplet's impact velocity may effect the spreadfactor.

3.4.4 *Advantages and Disadvantages of Method*

There are advantages and disadvantages to the use of either ultraviolet/visible or fluorescence spectroscopy. The former method is not sensitive enough for measuring small dye concentrations, but it is less susceptible to error due to solvent contaminations. The latter can easily measure small dye concentrations, but it very vunerable to minute contaminants (dust, residue left after solvent evaporation, dissolved solids, etc.). Ultra-pure solvents are required for accurate fluorescence measurements of solutions with low dye concentrations. In the present work, both ultraviolet/visible and fluorescence spectroscopy were employed for greater experimental accuracy and to compare the merits of each.

The general principle of the method, the use of tracer dyes/spectroanalysis to measure drop size, should be applicable to other simulant/dye/witness card combinations besides the one combination actually tested. Other combinations

should meet the following minimum requirements: the necessary criteria for accurately measuring stain sizes on witness cards (see Section 2.1); and, the suitability of the tracer dye for spectroanalysis.

Possible limitations that a simulant/dye/witness card combination may encounter for use in the present method are determining an appropriate solvent for dye extraction, possible fluorescence or UV/visible spectra interference from the simulant and/or thickener, fluorescence background interference from the witness card, and dye photostability. Consequently, the applicability of the present method must be evaluated on a case by case basis for other specific simulant/dye/witness card combinations.

However, the major advantage to the present method is that now the spreadfactor relationship can be directly deduced from the sample stains of an actual field trial (see Section 2.3). This eliminates the need to match the actual environmental conditions of the trial within the laboratory when determining the spreadfactor.

4. *PHASE II--APPLICATION OF METHODOLOGY IN THE EVALUATION OF DROPLET EVAPORATION DURING FREE FALL*

4.1 *Introduction*

With the use of a fluorescent tracer/witness cards, it is also possible to estimate the amount of droplet evaporation during free fall. Both Newtonian and non-Newtonian viscoelastic droplets can be evaluated, though the later presents unique obstacles. To measure evaporation, only the initial (D_{di}) and final (D_{df}) droplet diameters need to be known (see Diagram 1 for definition of terms):

$$(2) \qquad R_c = 100 \left(\frac{D_{df}}{D_{di}} \right)^3$$

with R_c being the % mass recovered (or 100% minus the mass lossed through evaporation). Both D_{di} and D_{df} can be measured using the method discussed in the present work: D_{di} from the amount of tracer dye recovered and measured spectroscopically, and D_{df} from the resulting stain size upon droplet impact.

The measurement of the evaporation of a viscoelastic (polymer thickened) liquid is complicated by the variation of fluid rheology as the polymer concentration increases during evaporation. It has been observed by the authors (and will be discussed in a future work) that the effect of the changing rheology on the spreadfactor relationship (D_d versus D_s) depends on the type of witness card material used. For materials of low absorpency (having little wicking effect on liquids), the effects of varying liquid rheology will be small. D_s, with such materials, is more dependent on the spreading caused by the initial droplet impact upon the witness card rather than on the subsequent wicking out of the liquid after impact. For materials of high absorpency, the opposite is true: the subsequent wicking out of the liquid after impact can greatly contribute to the final value for D_s. This phenonmena surrounding highly absorpent material is of particular interest, since witness cards composed of such material are commonly employed in open-air liquid dissemination trials.

When materials of high absorpency are used and significant droplet evaporation occurs, the droplet diameter upon impact, D_{df}, cannot be directly determined from D_s using the spreadfactor obtained under non-evaporative conditions. However, by knowing the initial droplet diameter, D_{di}, the effects of liquid rheology on the spreadfactor, as well as D_s, D_{df} can be successfully determined.

D_{di}, which is equal to D_{df} under non-evaporative conditions is found through the use of a dye tracer in the test liquid employed, in conjuction with the methodology discussed in Phase I of the present work. Liquid rheology effects are evaluated throught the creation of control stains using solutions of varying polymer concentrations.

4.2 *Experimental Method*

4.2.1 *Test Solution*

A polymer-thickened solution of DEM was prepared in a manner similar to that described in Section 3.2.1 except that a concentration of 4.0 g/dl, instead of 3.5 g/dl, K-125 polymer in DEM was used. The amounts of the tracer dyes used previously were not changed. However, in an attempt to prevent or lessen possible damage to the tracer dyes due to solar exposure, an ultra-violet absorber, 2,4-Dihydroxybenzonephenone (DHBP) (sold under the trade name of Syntase 100

by Neville-Syntheses Organics, Inc., Pittsburgh, PA), was added to the solution, with a nominal concentration of 2 wt. %.

4.2.2 *Test Procedure*

Droplets of the DEM/K-125 solution were atomized from a height of 55 meters above an array of witness cards. The material used for the witness cards was heavy blotter paper, 0.5 mm thick, supplied by Thomas Scientific, Swedesboro, NJ. The impacted cards were allowed to dry, and selected stains were later sized using the Quantimet 920 Image Analyzer (see Section 3.2.2). The tracer dyes were extracted from the stains using acetone and quantified using the fluorescence spectrophotometer. D_{di} was then determined from the amount of dye extracted. The analytical procedure used was the same as the one described in Section 3.2.3

At the same time the trial stains were being generated, three series of control stains were made upon blotter paper at the test site with a hand sprayer. The control stains were analyzed in the same manner as the trial stains. Three different DEM solutions, with polymer concentrations of 4.0, 5.7, and 7.6 g/dl, were used in order to evaluate polymer spreading effects. Because the solutions were sprayed slightly above the cards (and hence a small droplet settling time), no evaporation during free fall was assumed.

4.3 *Results*

4.3.1 *Experimental Data and Analysis*

Figure 9 shows the D_{di} versus D_s results obtained for a trial conducted at 69°F. Also indicated is the best fit regression of the 18 stains analyzed (dashed line) to similar results obtained from the same solution atomized directly above the witness cards (i.e. no evaporation). A comparison of the trial results with the regression for non-evaporation clearly indicates significant evaporation for D_{di} values less than 350 microns.

Figure 10 shows a plot of D_{di} versus D_s for the control stains and best fit regressions obtained for the three different polymer concentrated (i.e. 4.0, 5.7, and 7.6 g/dl) solutions sprayed slightly above the cards. A total of 47 stains were

FIGURE 9

Initial Droplet Diameter vs. Stain Diameter
Test Conducted Using DEM and Blotter Witness Cards

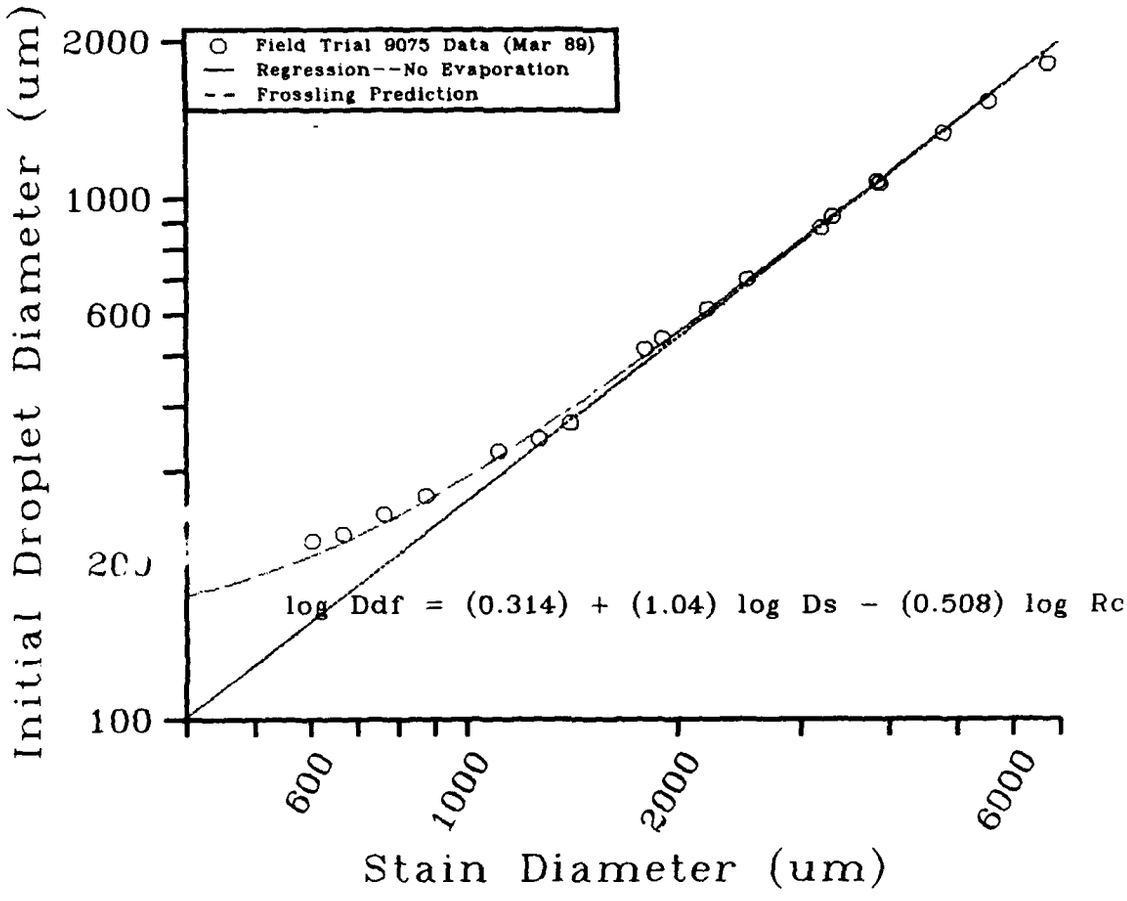

FIGURE 10

Reference Spreadfactor Curves as Function of Rc
For Stains Made with DEM on Blotter Paper

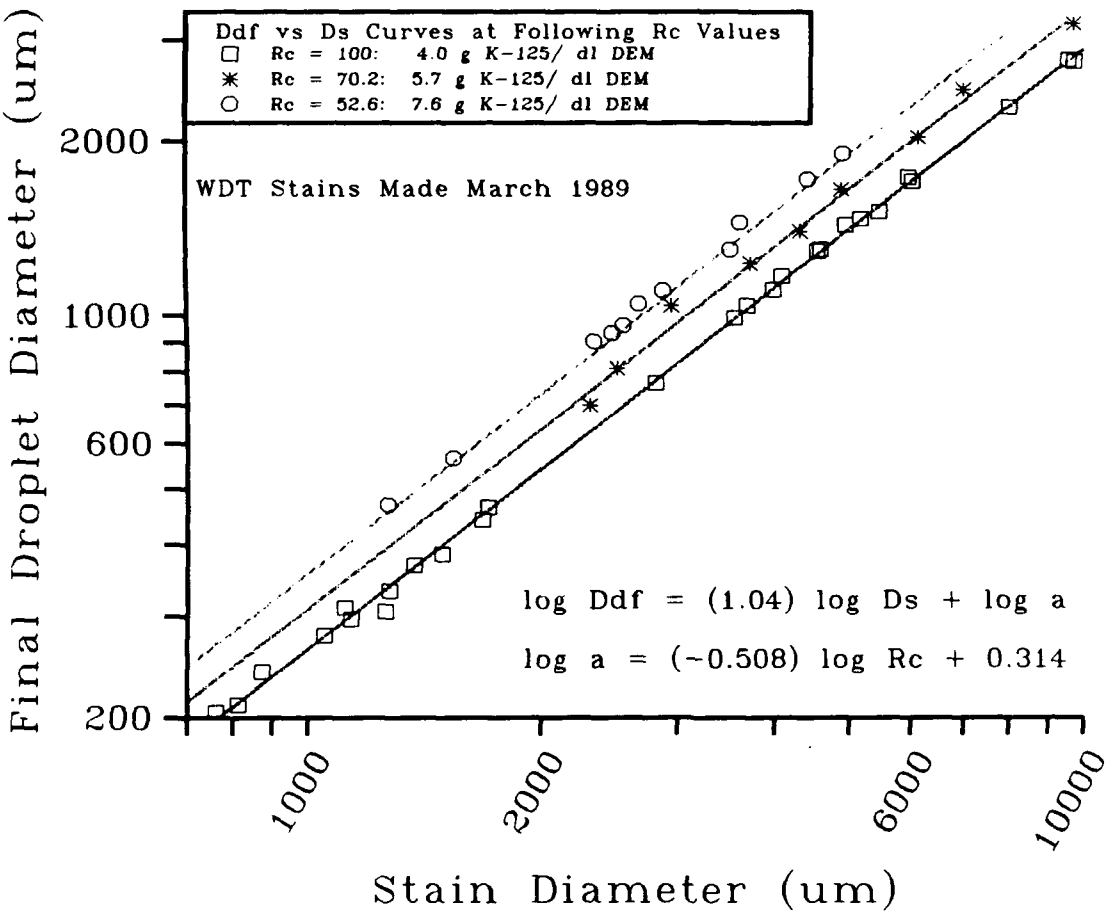

analyzed: 27 stains from the 4.0 g/dl solution, 10 from the 5.7 g/dl solution, and 10 from the 7.6 g/dl solution. No evaporation during free fall is assumed, thus for these reference stains, D_{di} is equal to Df. Since an 4.0 g/dl solution was dispersed for the evaporation trial, the 4.0, 5.7, and 7.6 g/dl control stains regression correspond to 0, 29.8, and 47.4% evaporation of the trial solution. The three regressions clearly indicate that droplet spreading decreases with increasing polymer concentration. The data presented in both Figures 9 and 10 are presented in more detail in Appendix E.

By relating the three variables, D_{df}, D_s, and R_c (which is equal to 100% minus % evaporation loss), together using a multiple variable correlation (see Appendix B for the mathematics involved and the computer programing employed), the following relation was derived:

$$(3)\quad \log_{10} D_{df} = a + b \log_{10} D_s - c \log_{10} R_c$$

with,

$$a = 0.314 \pm 0.039 \qquad b = 1.040 \pm 0.0064 \qquad c = -0.508 \pm 0.016$$

The fit of the above three dimensional relation to the experimental data is excellent, with the square of the correlation coefficient being equal to 0.998.

In order to use Eq. (3) towards calculating droplet evaporation for an actual field trial, Eq. (2) must be used to substitute D_{di} for D_{df}. Upon the subtitution of Eq. (2) into Eq. (3) and rearranging, the following is arrived at:

$$(4)\quad R_c = \left\{ 9.57 \left(\frac{D_s^{1.04}}{D_{di}} \right) \right\}^{1.19}$$

Table 2 provides a summary of the % Recoveries measured for Ddi values less than 350 microns. Also presented for comparison is the predicted % Recoveries obtained using a proprietary computer code employing the Frossling expression to determine the evaporational losses of a free-falling droplet.[7] For a detailed discussion of the Frossling expression, the reader is referred to the general overview of the evaporation of airborne droplets presented by Davies.[8]

TABLE 2

Comparison of Measured and Predicted R_c Values

D_{di} (μm)	D_s (μm)	R_c Measured	R_c Frossling
220	604	65.5	75.2
227	668	71.7	77.2
248	764	76.3	81.9
268	876	82.5	85.2
327	1113	87.7	91.0
345	1273	97.4	92.1

Exact R_c values were obtained from the computer coded Frossling expression in the following manner. Given a value for D_{di}, as well as the appropriate atmospheric conditions of the field trial, physical properties of the droplet, and total length of the fall, the computer code would calculated D_{df} upon impact. Using Eq. (2), R_c would then be calculated as shown in Table 2.

The Frossling prediction as shown in Figure 9 was prepared by determining D_s using Eq. (3) from known D_{df} and R_c values obtained from the computer code and Eq. (2). The resulting values for D_s as a function of D_{di} were then plotted, as seen in Figure 9.

4.3.2 *Error Analysis*

Due to the complexity of Eq. (3) and the statistical correlation among the equation constants, a straight forward determination of the error in a calculated R_c from the measured quantities D_{di} and D_s is not readily possible. In order to arrive at a reasonable error estimate, the Monte Carlo Method was used to determine the random error in R_c based upon the random errors associated with the constants and parameters of Eq. (3). The exact procedure employed, as well as the results obtained from, the Monte Carlo is presented in greater detail in Appendix C.

For the Monte Carlo Method, the following assumptions were made: 1.) the random error involved for the constants, a, b, and c is that determined from the multiple regression analysis performed to arrive at Eq. (3); 2.) the generation of

random values for the constants had to account for the correlation between a and b, and a and c (which was done by using the appropriate correlation coefficient as determined from the regression analysis); 3.) the random error in D_s, ΔD_s, is $\pm$ 35 μm; and 4.) the random error in D_{sf}, ΔD_{sf}, is $\pm$ 10 μm. The results obtained with these assumptions are shown in Table 3 on a linear basis instead of logrithmic.

TABLE 3

Monte Carlo Simulation Error Estimates for R_c Obtained from Eq. (3)

			Set I			Set II		
	ΔD_s (μm)			0			30	
	ΔD_{sf} (μm)		1	10	30	1	10	20
D_s (μm)	R_c (%)	D_{sf} (μm)		ΔR_c (%)			ΔR_c (%)	
500	50	181	5.0	7.9	21.1	9.3	11.5	16.1
	100	128	10.4	21.1	62.2	19.1	25.9	46.2
1000	50	372	5.0	6.0	10.4	6.4	6.8	8.5
	100	262	10.9	13.8	29.1	13.5	15.9	20.5
5000	50	1979	5.5	5.5	5.7	6.1	5.7	5.8
	100	1391	11.9	12.7	13.2	12.5	12.5	12.7

For the purpose of comparison, the error in D_s and D_{sf} was varied in order to check the sensitivity of the resulting absolute error in R_c, ΔR_c, is to any change in the accuracy of the two parameters. These results are also presented in Table 3.

Set II and the column for $\Delta\ D_{sf} = 10$ is the situation that was encountered in the present study. The % error (the ratio of ΔR_c to R_c) for this column ranges from 11 to 26%, with the larger measured D_s values giving the more accurate R_c values. However, significant evaporational losses in the present work were seen when D_s was less than 1500 μm. Thus, the approximate error range is defined by the Monte Carlo results for the pairs $D_s = 1000$ at $R_c = 100\%$, and $D_s = 500$ at $R_c = 50\%$, which corresponds to a % error range of 16 to 23%.

The error in R_c is not signficantly affected by changes in $\Delta\ D_{sf}$ and $\Delta\ D_s$ for any individual D_s values above 1000 μm. However, for D_s values less than 1000 μm, this is not the case. Obviously by reducing $\Delta\ D_{sf}$ and $\Delta\ D_s$ would greatly

improve the accuracy in measuring R_e, but the best that could be achieved would those error values found in the first column of Set 1 in Table 2, with the error in R_e ranging from 10 to 12%.

4.4 *Discussion*

It is evident from Figure 9 that the trial data is in agreement (within experimental error) with the predicted values from the Frossling equation. Accurate measurement of droplet evaporation under field trial conditions was achieved with the spectroscopy method of droplet sizing.

The potential for further improvement in the accuracy of the method is possible by reducing ΔD_s through the use of a higher magnification on the Quantimet 920. Also, the effect of ΔD_s and ΔD_{di} can be reduced through the analyzing of many stain samples. However, a point of diminishing returns will be reached quickly. It is doubtful that the effort required to gain the 4-5% additional accuracy would be economical.

The best approach to making the methodology more accurate would be to eliminate the need of generating calibration stains to account for effect of changing rheology (resulting from droplet evaporation) on the spreadfactor. By doing this, a multiple regression involving R_e would not be needed, thereby reducing Eq. (3) to a simple linear regression, which would be inherently more accurate than a multiple regression.

The need for calibration stains can be eliminated by using a witness card material where the spreadfactor relationship is independent of any change in liquid rheology. Materials possessing a low liquid absorpency (small wicking effect) would be ideal for such a purpose (see Section 4.1).

5. *CONCLUSIONS*

The droplet spreadfactor relationship determined through fluorescent and UV/VIS dye tracers is accurate and reliable for the polymer thickened (viscoelastic) DEM solution tested. The methodology can determine the spread factor relationship from stains obtained directly from an actual field dissemination trial without having to attempt to approximate field conditions in the

laboratory. Thus, the accuracy in determining drop size distributions and mass values in dissemination studies can be greatly improved over previous methods involving the measurement of spreadfactors under laboratory conditions.

The novel application of the tracer dye methodology towards measuring the free fall evaporation of droplets (generated from a polymer thickened (viscoelastic) solution) under field trial conditions was found to be an accurate approach (16 to 23% error) for the simulant/witness card/tracer dye combination employed.

6. *RECOMMENDATIONS*

6.1 *Accuracy of Methodology and Dye Photostability*

The accuracy of the method is highly dependent on the photostability of the tracer dyes employed, since any degradation on their part due to solar exposure, aging, or setting, will produce erroneous results. For the present study, this problem was not a factor, due to the care exercised in the handling of the samples (ie. prompt sample analysis, limited solar exposure of samples, etc.). Thus, it is recommended that the stains be promptly analyzed when there is doubt about the tracer dye's photostability.

The long-term effects of solar exposure, aging and setting on the tracer dyes employed is beyond the scope of this work. However, it is recommended that further studies be conducted to find an estimate of the "shelf life" (the length of time following stain creation before dye degradation affects the method's accuracy) of any tracer dye to be used for this method. Studies involving the dyes used in the present study are to be published in a future work.

To detect for solar degradation in the actual trial stains, it is recommended that a close comparison be made between the actual trial stains and (if made) the calibration stains generated at the time of the trial. The spreadfactor of the calibration stains, not being exposed to sunlight but still subjected to other field trial conditions (humidity, temperature, etc.), will not correspond to the spreadfactor of the actual trial stains should significant amount of solar degradation occur. However, this approach will not detect the affects of dye aging or setting (if not dependent on solar exposure) since both calibration and trial stains will be effected equally.

6.2 *Calibration Stains*

A series of calibration curves as used in Phase II of the present study are only needed whenever changes in the droplets' rheology, if they should occur, (see Section 4.1 for example) affects the spreading of the droplet in the witness card after impact. Otherwise, only one calibration curve is needed for determining the spreadfactor.

As shown in Phase II, the use of high absorpency witness cards can require the generation of a series of calibration stains, particularly if polymer-thickened (viscoelastic) fluids are involved. To avoid this problem, it is recommended that low absorpency witness cards be used whenever practical, thereby eliminating the need for a series of calibration curves and improving the accuracy in measuring the amount of any free fall evaporation that does occur (see Section 4.4).

When generating calibration stains, it recommended that a hand sprayer, rather than the WDT, be used to generate the droplets. This will eliminate the need to compensate for the possible effect of the droplet impact velocity on the calibration spreadfactor, since droplets generated by the sprayer will approximately be at the velocity as the trial droplets (terminal velocity).

However, if the WDT must be used (ie. no hand sprayer available), then only high absorpency witness cards (ie. Whatman #1 Filter Paper or a similar type) should be used for both calibration and trial stains. Under such conditions, the WDT droplets (zero velocity) spreadfactor will be the same as that from the trial droplets (terminal velocity), with all other factors being equal (see Section 3.4.3). Should significant amounts of free fall evaporation occur, then several calibration curves will have to be prepared as was done in Phase II.

LITERATURE CITED

1. Barry, John W., et. al., *"Methods For Sampling and Assessing Deposits of Insecticidal Sprays Released Over Forests"*. **Technical Bulletin No. 1596,** USDA Agriculture Forest Service, Davis CA, November 1978.

2. Sommerville, D. R., and J. E. Matta, *"Spectroscopically Derived Spreadfactors for Different Bacillus Thuringiensis Insecticidal Formulations on Paper Impaction Cards"*. USDA Forest Service Report, To be published.

3. Matta, J. E., R. P. Tytus, and J. L. Harris, *"Aerodynamic Atomization of Polymeric Solutions"*, **Chemical Engineering Commun. 19:** 191-204, 1983.

4. Davis, J. M., *"A Vibrating Apparatus for Producing Drops of Uniform Size."* **USDA Bur. Entomol. and Plant Quarterly**. ET-295, United States Department of Agriculture, 1951.

5. Maksymiuk, B. and A.D. Moore, *"Spread Factor Variation for Oil-Based, Aerial Sprays."* **Journal Econ. Entomol.** 55(5): 695-699, 1962.

6. May, K.R., *"The Measurement of Airborne Droplets by the Magnesium Oxide Method."* **Journal of Scientific Instrum.** 27: 128-130, 1950.

7. Frossling, N., **Gerlands Beirtage Geophys., 52,** 170-216, 1938.

8. Davies, C.N., *"Evaporation of Airborne Droplets,"* **Fundamentals of Aerosol Science.** ed. by D.T. Shaw, John Wiley and Sons, pp. 135-164, 1978.

9. *"Minitab Release 5.1,"* **Minitab, Inc.**, 1985.

10. Spiegel, M.R., *"Statistics,"* **Schaum's Outline Series.** McGraw Hill, 1961.

11. Meyer, S.L., **Data Analysis for Scientists and Engineers.** John Wiley and Sons, New York, 1975.

Blank

APPENDIX A

INSTRUMENT DESCRIPTION/OPERATING PARAMETERS AND DYE CHARACTERISTICS

A-1. *INSTRUMENT DESCRIPTION/OPERATING PARAMETERS*

A-1.1 *Perkin-Elmer Lambda 9 UV/VIS/NIR Spectrophotometer*

The Lambda 9 Spectrophotometer is a double-beam, double-monochromator and ratio recording device. It uses as a source a prealigned tungsten-halogen lamp for Near UV/VIS range (319.2 to 860.8 nm) and a side window photomultiplier detector.

In the present work, the following instrument parameters were used for measuring dye absorbance:

a. Slit width: 2.00 nm
b. Response Time: 0.5 seconds
c. Cell pathlength: 10 mm
d. Sample Temperature: 25°C
e. Sample Volume: 3 ml

A-1.2 *Perkin-Elmer Model LS-3B Fluorescence Spectrophotometer*

The LS-3B Spectrophotometer is a fluorescence spectrophotometer with separate excitation and emission scanning monochromators. It uses a pulsed xenon flash tube as a source, and a spectrally compensated signal is obtained by directing the reference beam through the a built-in triangular cell containing a solution of Rhodamine 101 dye. The whole system operates in a pulse mode with a short duty cycle; the source is pulsed and the detectors are gated at line frequency.

In the present work, the following instrument parameters were used for measuring dye fluorescence:

a. Slit width–
   Emission: 10 nm
   Excitation: 10 nm
b. Response Time: 4.0 seconds
c. Integration Time: 8.0 seconds
d. Cell Pathlength: 10 mm
e. Sample Temperature: 25°C
f. Sample Volume: 25 ml

A-2 *DYE CHARACTERISTICS*

A-2.1 *Tinopal SWN Dye*

Tinopal SWN Dye is the trade name for 7-diethylamino-4-methyl coumarin (DEAMC), a fluorescent whitening agent formally manufactured by the Ciba-Geiby Corporation. DEAMC is currently being manufactured by several other companies, the most notable being American Cyanamid Coroporation under the trade names of Calcofluor White RW and Calcofluor White RWP. As determined in the present study, DEAMC's major absorbance peak in acetone is located at a wavelength of 366 nm, and maximum fluorescence intensity is achieved at an excitation wavelength of 366 nm and an emission wavelength of 426 nm. At 366 nm, it has an absorbance per dye concentration value of 0.107 A/(ug/ml dye).

A-2.2 *Ceres Blue ZV Dye*

Ceres Blue ZV Dye is a dye of the Anthraquinone chemical family manufactured by Mobay Chemical Corporation, with the chemical name of the active ingredient being a trade secret. As determined in the present study, its major absorbance peaks in acetone are located at 598 and 645 nm. At these two peaks it has absorbance per dye concentration values of 0.0364 A/(ug/ml) and 0.0430 A/(ug/ml), respectively. Ceres Blue ZV Dye also has a broad absorbance band in the near ultra-violet region, overlapping the major UV absorbance peak of Tinopal SWN Dye. When used in approximately an 2:1 mass ratio with Tinopal SWN Dye, Ceres Blue ZV Dye contributes approximately 0.01 A/(ug/ml of Tinopal).

A-2.3 *Syntase 100 UV Absorber*

Syntase 100 is the trade name for 2,4-Dihydroxybenzonephenone (DHBP), which is manufactured by the Neville-Synthese Organics, Inc., Pittsburgh, PA. From 250 to 400 nm, the absorbance of DHBP is substantial. At 366 nm, the major absorbance peak of DEAMC, DHBP has an absorbance per unit concentration value of 0.013 A/(ug/ml) in acetone, approximately 1/8 the value for DEAMC.

A-3. *INSTRUMENT CALIBRATION PROCEDURES*

A-3.1 *Calibration Curve--Dye Concentration Versus Instrument Reading*

In order to determine the amount of dye recovered from a stain (and hence determine the mass of the original droplet), a calibration curve first had to be prepared for use with the Perkin-Elmer spectrophotometers. Two approaches were used to equate the concentration of dye present in the acetone solution (used to recover the dye) to the resulting absorbance and/or fluorescence reading obtained by the spectrophotometers.

Initially for Phase I (Evaluation of the Spectroscopy Approach--Section 3), data for a calibration curve was obtained by preparing acetone/dye solutions using known quantities of dye. Thus, the resulting curve was expressed as dye concentration as a function of instrument reading. In order to convert the dye concentration value into the desired droplet mass value, the % dye present in the orginal DEM solution had to be known. This was determined by subjection known amounts of the DEM solution to spectroscopic analysis and using the previously described calibration curves.

Since CBZV does have a broad absorbance band in the region of DEAMC's major absorbance peak, care was taken to maintain that the ratio of DEAMC and CBZV present in the calibration solutions were approximately equal to ratio present in the the actual thickened DEM solutions used in the present study. Since only two absorbing components were involved, preparation of calibration solutions with the proper dye ration was not difficult.

However, for Phase II of the present study (Application of Methodology Towards Droplet Evaporation), the addition of Syntase 100 complicated the preparation of the calibration solutions, due to its significant contribution to the absorbance at 366 nm (DEAMC's primary peak).

A-3.2 *Quality Assurance Measures Taken for the Analytical Instruments*

The fluorescent intensity that is emitted by (and detected for) a particular sample in a fluorescence spectrophotometer is proportional to the energy output from the instrument's light radiation source. If this is not accounted for by the use of standards or very frequent up-grading of calibration curves, errors in measuring fluorescence could easily occur.

In order to analysis two or more fluorescence data sets taken on different days, the effects of the changing energy output of the source had to be accounted for. This was done through the use of solid fluorescence standards provided by the Perkin-Elmer Company for use in their instruments. These standards consisted of polymethylmethacrylate (PMMA) blocks impregnated with various fluorescent dyes. The PMMA provides stability to the dyes, so that any changes in fluorescence intensity is instrumental rather than chemical in nature.

Thus, the PMMA blocks were used to "correct" sample measurements to that of a calibration curve by using the ratio of the intensity reading of the PMMA blocks taken at the time of the sample to that taken at the time of the calibration curve. By taken reading of the PMMA blocks frequently (between each or every other sample), even source variations over a short time period could be effectively account for in their effect on intensity readings.

APPENDIX B

USE OF A MULTIPLE CORRELATION/REGRESSION FOR A THREE VARIABLE SYSTEM

B-1. INTRODUCTION

The degree of relationship existing between three or more variables is defined as a multiple correlation, with the fundamental principles of multiple correlation being analogous to those of simple (or binary) correlation.[10] These analogous equations permit the statistical determination of the relationship between D_d, D_s, and % Recovery (see Figure 2). The following presents the equations employed to determine this relationship, which were obtained from Schaum's Outline on Statistics.[10] Only a brief review of the equations' derivation is presented in this appendix. A more complete description can be obtained from the cited work. For convenience, the notation used in Schaum's is employed in this appendix.

For ease of calculation, a general purpose data analysis system, MINITAB,[9] was employed to perform the necessary calculations as outlined in Sections B-2 through B-4. The results given by this program are provided in Sections B-5 and B-6.

B-2. MULTIPLE CORRELATION

For three variables, the simplest regression of X_1 on X_2 and X_3 has the form:

$$(B1) \quad X_1 = b_{1.23} + b_{12.3}X_2 + b_{13.2}X_3$$

where $b_{12.3}$, $b_{1.23}$, and $b_{13.2}$ are constants.

Eq. $(B1)$ represents a regression plane. By keeping either X_2 or X_3 constant, Eq $(B1)$ reduces to the familiar two-variable or binary correlation having a line equation representation. The key to performing a least square regression on a trinary system is to first perform a regression on each the three

binary systems (the pairs X_1 and X_2, X_1 and X_3, and X_2 and X_3) obtained by holding one variable constant. Using zero order correlation coefficients (r_{12}, r_{13}, and r_{23}) and the standard deviations of X_1, X_2, and X_3 (s_1, s_2, and s_3) obtained from the individual binary regressions, the following least square regression plane can be derived:

$$(B2) \quad \left(\frac{x_1}{s_1}\right) = \left(\frac{(r_{12} - r_{13}r_{23})}{(1 - r_{23}^2)}\right)\left(\frac{x_2}{s_2}\right) + \left(\frac{(r_{13} - r_{12}r_{23})}{(1 - r_{23}^2)}\right)\left(\frac{x_3}{s_3}\right)$$

where $x_i = X_i - (\Sigma X_i/N)$, and N is the total number of data points. Substituting in for x_i and rearranging, the following is derived:

$$(B3) \quad X_1 = d_1X_2 + d_2X_3 + (1/N)\left[\Sigma X_1 - (d_1\Sigma X_2) - (d_2\Sigma X_3)\right]$$

where,

$$(B3.1) \quad d_1 = \left(\frac{(r_{12} - r_{13}r_{23})}{(1 - r_{23}^2)}\right)\left(\frac{s_1}{s_2}\right)$$

$$(B3.2) \quad d_2 = \left(\frac{(r_{13} - r_{12}r_{23})}{(1 - r_{23}^2)}\right)\left(\frac{s_1}{s_3}\right)$$

r_{ij} and s_i are defined as:

$$(B4) \quad r_{ij}^2 = \frac{\left\{N(\Sigma X_iX_j) - (\Sigma X_i)(\Sigma X_j)\right\}^2}{\left\{N(\Sigma X_i^2) - (\Sigma Xi)^2\right\}\left\{N(\Sigma X_j^2) - (\Sigma X_j)^2\right\}}$$

$$(B5) \quad s_i^2 = \left(\frac{(\Sigma X_i^2)}{N}\right) - \left(\frac{(\Sigma X_i)^2}{N^2}\right)$$

For a least square regression plane, the standard error of estimate, $s_{i.jk}$, and the coefficient of linear multiple correlation, $R_{i.jk}$, are defined as:

$$(B6) \quad s_{i.jk}{}^2 = s_i{}^2 \left\{ \frac{\left(1 - r_{ij}^2 - r_{ik}^2 - r_{jk}^2 + (2r_{ij}r_{ik}r_{jk})\right)}{(1 - r_{jk}^2)} \right\}$$

$$(B7) \quad R_{i.jk}{}^2 = 1 - (s_{i.jk}/s_i)^2$$

B-3. METHOD OF COMPUTATION

The following procedure should be followed in order to arrive at the final regression plane for a set of experimental data points:

1. Calculate all $\sum X_i$, $\sum X_i X_j$, and $\sum X_i^2$ values for the set (a total of 9 values in all for a three variable data set).

2. Calculate r_{ij} using Eq. $(B4)$.

3. Calculate s_i using Eq. $(B5)$.

4. Using the results of Steps 2 and 3 in Eq. $(B3)$ arrive at the final form for least square regression plane.

5. Calculate $s_{i.jk}$ using Eq. $(B6)$.

6. Calculate R_{ijk} using Eq. $(B7)$.

B-4. APPLICATION OF MULTIPLE CORRELATION TO PRESENT STUDY

B-4.1 Experimental Variables of Interest

In the present study, the following substitutions were made for X_i:

$$(B8.1)\ X_1 = \log_{10} D_s \qquad (B8.2)\ X_2 = \log_{10} D_{df} \qquad (B8.3)\ X_3 = \log_{10} R_c$$

where R_c is the percent recovery of the liquid after evaporation. Upon the substitution of Eq. $(B8)$ into Eq. $(B3)$, a equation of the form similar to Eq. $(B1)$ is obtained. Comparison of the two equations shows that the constant "a" in Eq. (1) is dependent on R_c.

B-4.2 Correlation of Control Stain Data

As explained in the main sections of the present work, three sets of control stains were generated at the same time (in such a manner to avoid evaporation) that the actual field trial was being conducted. The stains were generated using 4.0, 5.7, and 7.6 g/dl K- 125/DEM solutions, having corresponding R_c values of 100, 70.2, and 52.6 percent, respectively. Thus, each set of D_s and D_{df} values for an individual stain was paired with the appropriate R_c value depending on the polymer solution used to generate that particular stain. After tabulating the data in the form of D_s, D_{df}, and R_c values per datum, the procedure for multiple correlation was followed as outlined in Sections B-2 and B-3.

B-4.3 Calculation of Individual Droplet Evaporation Losses

Since spectroscopy can only directly determine D_{di} (which is equal to D_{df} only when there is no evaporation), D_{di} must be substituted for D_{df} in order to use the equations of Section B-3 in conjuction with the spectroscopic spreadfactor. By doing this, R_c can be calculated directly. In logarithmic terms, D_{df} as a function of D_{di} can be expressed as (see also Eq. (2)):

$$(B9)\quad \log_{10} D_{df} = \log_{10} D_{di} - (2/3) + (1/3) \log_{10} R_c$$

Substituting Eqs. $(B8)$ and $(B9)$ into $(B3)$ and solving for R_c:

$$(B10)\quad \log_{10} R_c = \left(\frac{3}{3 + f_2}\right)\left(f_1 \log_{10} D_s - f_2 \log_{10} D_{di} + (2/3) f_2 + f_3\right)$$

where,

$$(B10.1)\quad f_1 = (1/d_1) \qquad (B10.2)\quad f_2 = (d_1/d_2)$$

$$(B10.3)\quad f_3 = f_2(\Sigma X_2/N) - f_1(\Sigma X_1/N) + (\Sigma X_3/N)$$

Eq. $(B10)$ can be simplified to,

$$(B11)\quad R_c = \left\{ a \left(\frac{D_e^b}{D_{di}} \right) \right\}^c$$

where,

$$(B11.1)\quad a = 10^{(2/3) + (f_3/f_2)}$$

$$(B11.2)\quad b = \left(\frac{f_1}{f_2} \right)$$

$$(B11.3)\quad c = \frac{1}{\left([1/f_2] + [1/3] \right)}$$

B-5. USE OF COMPUTER PROGRAM FOR REGRESSION ANALYSIS

In order to perform the calculations outlined in Sections B-2 through B-4, the computer program, MINITAP, was employed. Outlined in Section B-6 are the computer code, results printout, and the data file used by MINITAB in its regression analysis. The program output concerning the error associated with the regression analysis (Section B-6.3) are subsequently used in the Monte Carlo Simulation presented in Appendix C. Except for section headings, the information in Section B-6 is formated in the same manner as it was printed out by MINITAB.

B-6. PRINTOUT OF COMPUTER CODE USED WITH AND RESULTS OBTAINED FROM MINITAB DATA ANALYSIS SYSTEM

B-6.1 Computer Code Employed

```
MTB > exec 'rs'
MTB > let c4=logten(c1)
MTB > let c5=logten(c2)
MTB > let c6=logten(c3)
MTB > regr c5 2 c4 c6 c7-c8;
SUBC> vif;
SUBC> xpxinv m1;
SUBC> mse k1.
```

B-6.2 Results (See Also Section 4.3.1)

The regression equation is

$$(3)\quad \log_{10} D_{df} = 0.314 + 1.04 \log_{10} D_s - 0.508 \log_{10} R_c$$

		Eq. (3)			
Predictor	Coef	Constant	Stdev	t-ratio	VIF
Constant	0.31384	a	0.03947	8.10	
logDs	1.03857	b	0.00635	163.53	1.0
log%R	-0.50794	c	0.01627	-31.23	1.0

s = 0.01304 R-sq = 99.8% R-sq(adj) = 99.8%

Analysis of Variance

SOURCE	DF	SS	MS
Regression	2	4.8842	2.4421
Error	44	0.0075	0.0002
Total	46	4.8917	

SOURCE	DF	SEQ SS
logDs	1	4.7183
log%R	1	0.1659

Unusual Observations

Obs.	logDs	logDdf	Fit	Stdev.Fit	Residual	St.Resid
21	3.10	2.48430	2.52320	0.00331	-0.03890	-3.08R
28	3.36	2.84448	2.87595	0.00226	-0.03148	-2.45R
30	3.47	3.01662	2.98629	0.00213	0.03033	2.36R

R denotes an obs. with a large st. resid.

MTB > end

B-6.3 Calculation of Error in Regression Variables

MTB > print k1 m1
K1–Mean Square Error (MSE) 0.000170134

MATRIX M1–The p by p matrix INV(X',X)

9.15654	-0.91422	-3.12972
-0.91422	0.23706	0.04809
-3.12972	0.04809	1.55507

MTB > mult k1 m1 m2
MTB > print m2
MATRIX M2–The MSE*INV(X',X) matrix, known also as the variance-covariance matrix of coefficients.

$s_{x,y}$

x \ y	a	b	c
a	0.00155784	-0.00015554	-0.00053247
b	-0.00015554	0.00004033	0.00000818
c	-0.00053247	0.00000818	0.00026457

To find the correlation between a and the other two constants, b and c, the following equation should be used:

$$(B12)\quad r_{x,y} = \frac{s_{x,y}}{s_x\, s_y}$$

where $s_{x,y}$ can be obtained by crossing referencing a against b or c in MATRIX M2, and the individual s obtained from Section B-6.2 under the StDev column of the printout of the regression analysis results.

B-6.4 Listing of the Actual Data Values Used in MINITAB

MTB > print c4-c8

ROW	$\log_{10} D_s$	$\log_{10} D_{df}$	$\log_{10} R_c$	residual	predict
1	3.78204	3.23121	2.00000	-0.05316	3.23189
2	3.71567	3.16702	2.00000	0.32037	3.16295
3	3.77685	3.23855	2.00000	0.95367	3.22649
4	3.98200	3.44201	2.00000	0.19839	3.43956
5	3.90558	3.35946	2.00000	-0.05875	3.36019
6	3.98914	3.43949	2.00000	-0.60580	3.44697
7	3.69636	3.15564	2.00000	1.00214	3.14290
8	3.66342	3.11361	2.00000	0.38636	3.10869
9	3.73965	3.17898	2.00000	-0.70058	3.18786
10	3.23249	2.66558	2.00000	0.34919	2.66113
11	3.13735	2.56585	2.00000	0.27794	2.56233
12	3.22531	2.64345	2.00000	-0.80309	2.65368
13	3.17319	2.58433	2.00000	-1.19877	2.59954
14	2.91062	2.32222	2.00000	-0.37547	2.32685
15	3.04805	2.49136	2.00000	1.73462	2.46958
16	3.10585	2.51983	2.00000	-0.77499	2.52961
17	3.02160	2.44248	2.00000	0.02925	2.44211
18	2.94151	2.38021	2.00000	1.71635	2.35893
19	2.88195	2.30963	2.00000	1.02103	2.29708
20	3.05614	2.47129	2.00000	-0.53274	2.47799
21	3.09968	2.48430	2.00000	-3.08345	2.52320
22	3.44948	2.88309	2.00000	-0.26543	2.88649
23	3.55291	2.99520	2.00000	0.09998	2.99392
24	3.56785	3.01662	2.00000	0.56168	3.00943
25	3.60228	3.04454	2.00000	-0.05065	3.04519
26	3.61395	3.06707	2.00000	0.76453	3.05731
27	3.65916	3.10992	2.00000	0.44388	3.10426
28	3.36418	2.84448	1.84634	-2.45005	2.87595
29	3.40019	2.90795	1.84634	-0.42074	2.91336
30	3.47041	3.01662	1.84634	2.35695	2.98629
31	3.57322	3.08884	1.84634	-0.32795	3.09306
32	3.63749	3.14457	1.84634	-1.18741	3.15981
33	3.69046	3.21748	1.84634	0.20770	3.21483
34	3.78888	3.30835	1.84634	-0.68268	3.31703
35	3.84696	3.39076	1.84634	1.05889	3.37736
36	3.98807	3.50515	1.84634	-1.50565	3.52391
37	3.10312	2.67025	1.72099	0.14228	2.66850

38	3.18752	2.75128	1.72099	-0.39356	2.75615
39	3.36996	2.95472	1.72099	0.72636	2.94563
40	3.39375	2.96895	1.72099	-0.11089	2.97034
41	3.40807	2.98272	1.72099	-0.19846	2.98521
42	3.42813	3.01953	1.72099	1.07481	3.00605
43	3.45969	3.04297	1.72099	0.33009	3.03883
44	3.54728	3.11361	1.72099	-1.28953	3.12979
45	3.56015	3.16017	1.72099	1.35590	3.14315
46	3.64699	3.23452	1.72099	0.09328	3.23335
47	3.69223	3.27921	1.72099	-0.08977	3.28033

MTB > nooutfile

Blank

APPENDIX C

USE OF MONTE CARLO SIMULATION FOR ERROR ANALYSIS OF PHASE II RESULTS

C-1. *INTRODUCTION*

The Monte Carlo Simulation is a method for the determination of the expected variation in a calculated parameter through the generation of random "experimental" values upon which the parameter is based. A complete description of this method is beyond the scope of this work, though the reader is referred to a general text book which discusses the subject.[11] A short discussion of the basic theory involved is presented in this appendix. For the purpose of the present discussion, all random number generations are assumed to have a normal distribution of values.

C-1.1 *Theory for Independent Parameters*

In order to better explain the method, let Eq. (C1) be used as an example:

$$(C1)\quad A = B\,(\pm\Delta B) + C\,(\pm\Delta C)$$

By randomly generating values for B and C, different values are obtained for A. The range of typical "expected" values that are randomly generated for B and C can be made "realistic" by employing as the ranges' standard deviation, ΔB and ΔC, respectively for B and C. The resulting values obtained for A should then be "realistically" possible under normal conditions.

To arrive at an error estimate of A, the "normal" or mean A is calculated by using the means of B and C in Eq. (C1). Then, ΔA for each random A value (obtained through the generation of a random B and C value) is determined by taking the diffence between the mean of A and the random A value. By plotting individual ΔA values versus the value of their score function (see ref. 11 for more complete description of the score function), the resulting slope of the curve is equal to the maximum likelihood estimate of ΔA. The computer program MINITAB provides score function values through the use of the NSCORE command.[9]

C-1.2 *Theory for Correlated (Non-Independent) Parameters*

The procedure as explained in Section C-1.1 is valid only if B and C are not correlated with each other (ie. are independent of each other). In the present study, the parameters D_s and D_{df} are independently measured, and thus there is no correlation between them. However, for the constants of Eq. (3) (a, b, and c), this is not the case, since they were obtained simultaneously through a regression analysis, which by its very nature results in constants that are correlated to some degree with each other. Due to the interrelationship between the constants, random values cannot be independently generated for each. The following procedure was employed to account for this, using following equation as an example:

$$(C2)\quad X = (m \pm \Delta m)\, Y + (d \pm \Delta d)$$

with Y being a measureable quantity and m and d being experimentally derived constants with an associated standard deviation Δm and Δd, respectively. Let $r_{m,d}$ be the correlation coefficient between m and d (as defined by Eq. (B12)).

First, let a normal distribution of random numbers, D_1, (with a total of N values, mean of zero, and standard deviation of one, or $N(0,1)$), be generated for m (for the moment ignoring the true mean and standard deviation of m). Multiply $N(0,1)$ by $r_{m,d}$ produces a second distribution, D_2, equal to $N(0,r^2_{m,d})$. The correlation between D_1 and D_2 at this step is perfect, being equal to 1 or -1.

If a third distribution, D_3, is randomly generated, having N values, a mean of zero, and a standard deviation of Δd, $N(0,(\Delta d)^2)$, a set of perfectly correlated and a set of totally independent distributions are formed: D_1 and D_2, and D_1 and D_3, respectively.

By adding together D_2 and D_3, a fourth distribution, D_4 is formed, equal to $N(0,1)$, which is correlated to D_1 by the desired factor, $r_{m,d}$. Due to this correlation, it can be assumed that D_4 is an adequate random representation of d values correlated in the manner as m values. Mathematically, the addition of distributions can be expressed as:

$$(C3.1)\quad D_2 + D_3 = r_{m,d} D_1 + D_3 = D_4$$

or

$$(C3.2)\quad N(0,r_{m,d}^2) + N(0,(\Delta d)^2) = N(0,1)$$

since $(\Delta d)^2 = 1 - r_{m,d}^2$.

The mathematical proof that the random distributions, D_1 (for m values) and D_4 (for d values) are correlated by the factor of $r_{m,d}$ is as follows, using Eq. (B12) (with s_m being equivalent to Δm, likewise with s_d equal to Δd):

$$(B12)\quad r_{m,d} = \frac{s_{m,d}}{s_m\ s_d} = \frac{[(\Sigma md)/N]}{[(\Sigma m^2)/N]\ [(\Sigma d^2)/N]}$$

Since, s_m and s_d equal 1 (due to the manner of generation of D_1 and D_4), Eq. (B12) reduces to:

$$(C4)\quad r_{m,d} = (\Sigma md)/N = (\Sigma D_1 D_4)/N$$

Substituting for D_4 using Eq. (C3.1),

$$(C5)\quad r_{m,d} = \frac{\Sigma D_1(r_{m,d}D_1 + D_3)}{N} = \frac{r_{m,d}\Sigma {D_1}^2}{N} + \frac{\Sigma D_1 D_3}{N}$$

Since D_1 and D_3 are independent of each other and both have a mean of zero, $(SUMD_1D_3)/N$ is subsequently equal to zero, which then reduces Eq. (C5) to:

$$(C6)\quad r_{m,d} = \frac{r_{m,d}\Sigma {D_1}^2}{N}$$

By definition,

$$(C7)\quad s_m = \frac{\Sigma m^2}{N} = \frac{\Sigma {D_1}^2}{N}$$

So, since s_m equals 1, then substituting Eq. (C7) into Eq. (C6) leaves $r_{m,d}$ being equal to itself, thereby finishing the proof.

Having established two distributions, D_1 and D_4, for m and d, respectively, with the desired correlation, $r_{m,d}$, the next step is to establish the correct mean and standard deviation for both m and d in these distributions. This is done as follows, with $\overline{m}$ being the mean value for m:

$$(C8)\quad D_m = \Delta m D_1 + \overline{m}$$

The same is done for d by using D_4 and $\overline{d}$ instead of D_1 and $\overline{m}$. The two distributions, D_m and D_d, are then treated in the same manner as outlined in Section C-1.1 in order to arrive for an error estimate of X in Eq. (C2).

C-2 *APPLICATION OF MONTE CARLO THEORY TO PRESENT STUDY*

In the present study, the problem being examined is a combination of those discussed in both Sections C-1.1 and C-1.2. Measured independent values (such as B and C in Eq. (C1)) and the interdependency of experimentally derived constants (such as m and b in Eq. (C2)) are involved, with all the concerned values having an associated standard deviation.

The equation subjected to the Monte Carlo was a rearrange form of Eq. (3):

$$(C9)\quad \log_{10} R_c = \left(\frac{1}{c}\right)\left[a + \log_{10}\left(\frac{D_s^b}{D_{df}}\right)\right]$$

with,

$$a = 0.314 \pm 0.039 \qquad b = 1.040 \pm 0.0064 \qquad c = -0.508 \pm 0.016$$

Both the measured parameters, D_{df} and D_s, are independently measured and have associated with them a random error. For the purposes of the simulation, the error was estimated for each parameter based upon the conditions under which the measurements were made.

From Eq. (B12), the correlation coefficients between the pairs, ab, ac, and bc, were calculated and found to be -0.85, 0.62, and 0.04, respectively. Due to the low correlation between b and c, these two coefficients where assumed to be

independent of each other.

The first step in the generation of random values for the constants was to generate 300 random numbers for a, D_a. Then using the procedure outlined in Section C-1.2, random numbers were then generated for b and c (D_b and D_c) based upon their correlation with a. Upon the completion of the generation, the correlations between D_a with the other two distributions were check to ensure that the correlation was accurately reproduced.

After random numbers were generated for the constants, random numbers were generated for the measured parameters. Then using the procedure outlined in Section C-1.1, individual ΔR_c values were calculated for each random R_c value, which were then converted using the NSCORE function of MINITAB into the maximum likelihood estimate of ΔR_c.

In order to gain an understanding on how sensitive ΔR_c was to the magnitude of the measured parameter, as well as their error, different D_s, D_{df}, R_c, ΔD_s and ΔD_{df} values were employed. A total of 36 possible combinations were employed. The results of the Monte Carlo experiments are presented in Table 3 in Section 4.3. The actual computer code employed in presented in Section C-3.

C-3 *COMPUTER CODE EMPLOYED IN CONJUNCTION WITH MINITAB DATA ANALYSIS SYSTEM FOR MONTE CARLO SIMULATION OF PHASE II RESULTS*

The following is a listing of the actual computer code employed in the Monte Carlo Simulation of the Phase II results. The results of the program can be found in Table 3 in Section 4.3.

PROGRAM TRY.MTB

```
noecho
let k5=500
let k9=50
let k14=1
exec 'eqn1' 3
print k4 k14 k5 k9
let k5=1000
exec 'eqn1' 3
```

```
print k4 k14 k5 k9
let k5=5000
exec 'eqn1' 3
print k4 k14 k5 k9
let k5=500
let k9=100
exec 'eqn1' 3
print k4 k14 k5 k9
let k5=1000
exec 'eqn1' 3
print k4 k14 k5 k9
let k5=5000
exec 'eqn1' 3
print k4 k14 k5 k9
let k5=500
let k9=50
let k14=10
exec 'eqn1' 3
print k4 k14 k5 k9
let k5=1000
exec 'eqn1' 3
print k4 k14 k5 k9
let k5=5000
exec 'eqn1' 3
print k4 k14 k5 k9
let k5=500
let k9=100
exec 'eqn1' 3
print k4 k14 k5 k9
let k5=1000
exec 'eqn1' 3
print k4 k14 k5 k9
let k5=5000
exec 'eqn1' 3
print k4 k14 k5 k9
let k5=500
let k9=50
let k14=20
exec 'eqn1' 3
```

```
print k4 k14 k5 k9
let k5=1000
exec 'eqn1' 3
print k4 k14 k5 k9
let k5=5000
exec 'eqn1' 3
print k4 k14 k5 k9
let k5=500
let k9=100
exec 'eqn1' 3
print k4 k14 k5 k9
let k5=1000
exec 'eqn1' 3
print k4 k14 k5 k9
let k5=5000
exec 'eqn1' 3
print k4 k14 k5 k9
```

SUBROUTINE EQN1.MTB

```
noecho
OH=0
brief 1
##Monte Carlo Simulation to Estimate the Error in Calculating %
##Recovery of a Falling Droplet using Calibration Equation Derived
##from Test RS9075 conducted March 1989.
##k1=mean of a  k2=mean of b    k3=mean of c
##k11=stdev of a  k12=stdev of b  k13=stdev of c
##k4=mean of Ddf (final drop dia.)  k14=stdev of Ddf
##k6=total number of random numbers
##k7=corr. coefficient of a and b
##k17=corr. coefficient of a and c
##k8=stdev. of a and b
##k18=stdev. of a and c
##k9=% Recovery--R
##k19=logR
##k5=mean of Ds--Stain Diameter  k15=stdev of Ds
let k19=logten(k9)  ##Taking the log of % Recovery
##Calculating Ddf from set logR and logDs using calibration equation.
```

```
let k4=k1+(k2*logten(k5))+(k3*k19)
let k4=(10**k4)
random 300 c1  ##Random values generated for a--N(0,1)
##Establishing random numbers for b and c which are correlated to a
##by using the appropriate correlating coefficients.
mult c1 k7 c2  ##a--N(0,1)>>b--N(0,rab)
mult c1 k17 c3 ##a--N(0,1)>>c--N(0,rac)
##Calculating stdev for the correlating coefficients.
let k8=sqrt(1-(k7**2))  ##calculating s--s=sqrt(1-r**2)
let k18=sqrt(1-(k17**2))
random 300 c4;
normal 0 k8.    ##N(0,s**2)
random 300 c5;
normal 0 k18.   ##N(0,s**2)
add c4 c2 c2    ##N(0,s**2) + N(0,rab) = N(0,1)
add c5 c3 c3    ##N(0,s**2) + N(0,rac) = N(0,1)
##Taking the random numbers for a, b, and c, and converting them to
##real values for the constants by multiplying the columns of random
##numbers by the established means of a, b, and c.
mult c1 k11 c1
add c1 k1 c1
mult c2 k12 c2
add c2 k2 c2
mult c3 k13 c3
add c3 k3 c3
corr c1 c2  ##double check initial setpoint for k7 (correlation)
corr c1 c3  ##double check initial setpoint for k8 (correlation)
let c11=c1
let c12=c2
let c13=c3
random 300 c14;
normal mu=k4 sigma=(k14).  ##generating const. a b c Ddf and Ds
random 300 c15;
normal mu=k5 sigma=(k15).
##desc c11-c15
##let k9=(-1/k3)*(k1+logten((k5**k2)/k4))  ##calculating exact logR
let c8=(-1/c13)*(c11+logten((c15**c12)/c14))  ##calculating random
let c9=k19-c8
nscore c9 c10
```

```
regr c9 1 c10
##print k4 k14 k5 k15 k9
echo
```

Blank

APPENDIX D

EXPERIMENTAL DATA AND REGRESSION ANALYSIS RESULTS FOR PHASE I RESULTS

(See Also Section 3.3)

TABLE D1

Experimental Data Obtained from Spray Booth Stains

Set A--1 day				
D_s {μm}	D_d {μm} Based Upon Measurements From:			
	Fluor.	Absorbance at λ {nm}		
		366	598	645
737	254			
790	276			
1057	362			
1347	425			
1524	452			
1917	520			
2747	712			
3582	832	873	812	797
4172	975	1009	950	947
4189	968	984	932	921
4258	960	984	932	921
4364	1000	1027	972	972
4370	982	990	939	932
4833	1042	1057	1018	1011
4990	1102	1121	1074	1074
5726	1217	1240	1186	1181

D_v {μm}	D_d {μm} Based Upon Measurements From:			
	Fluor.	Absorbance at λ {nm}		
		366	598	645
Set B--3 days				
604	252			
816	252			
853	308			
1006	336			
1451	429			
1473	455			
1616	456			
1724	493			
3819	884	905	877	864
3884	879	913	851	846
3983	878	913	864	846
4142	898	935	889	877
4479	949	1015	961	947
4593	1009	1034	989	972
5244	1137	1165	1104	1099
7172	1420	1425	1405	1403
Set C--1 week				
709	252			
784	290			
978	313			
1247	393			
2042	497			
2298	626			
2341	620			
2348	598			
3871	952	882	851	855
4032	985	935	877	877
4251	998	984	950	947
4297	988	984	950	947
4499	999	997	950	939
4660	1029	1039	1008	1005
5200	1099	1100	1065	1060
5229	1082	1090	1051	1039

Set D--2 weeks				
D_s {μm}	D_d {μm} Based Upon Measurements From:			
	Fluor.	Absorbance at λ {nm}		
		366	598	645
610	421			
931	332			
935	325			
1344	406			
1800	508			
2076	580			
2773	660			
3546	821	781	788	777
3903	949	865	864	846
3991	899	921	851	846
4107	943	921	909	905
4363	961	943	932	932
4477	971	943	932	932
4543	1000	963	950	939
6148	1352	1353	1328	1321
6838	1359	1360	1343	1334
Set E--4 weeks				
900	291			
1057	336			
1124	361			
1379	404			
1804	487			
3054	691			
3278	735			
3561	1303	839	841	822
3777	1249	882	877	864
3813	881	873	851	846
3829	880	890	851	846
4081	893	898	889	885
4407	939	971	950	939
4798	1021	1039	1024	1027
5719	1145	1183	1172	1175
5861	1217	1248	1241	1233

Appendix D

TABLE D2

Results of Linear Regression Analysis of D_d vs. D_s

Set	a	b	r^2	$s_{y,x}$
A	0.743	0.291	0.998	0.0096
B	0.721	0.358	0.993	0.0201
C	0.747	0.273	0.992	0.0190
D	0.726	0.350	0.994	0.0148
E	0.737	0.293	0.997	0.0110
all	0.735	0.314	0.994	0.0170

For the following the relation:

$$\log_{10} D_d = a \log_{10} D_s + b$$

With r and $s_{y,x}$ being the correlation coefficient and the standard deviation of y on x, respectively.

To convert from drop diameter to drop mass, use the following relation:

$$mass = \pi \left(\frac{\rho}{6} \right) D_d^3$$

With ρ equal to 1.055 for diethyl malonate.

APPENDIX E

EXPERIMENTAL DATA AND REGRESSION ANALYSIS RESULTS FOR PHASE II RESULTS

(See Also Section 4.3.1)

TABLE E1

D_{di} and D_s Data for Droplet Evaporation Study
(Study Conducted March 1989)

D_s (μm)	D_{di} (μm)
604	220
668	227
764	248
876	268
1113	327
1273	345
1411	370
1797	514
1907	539
2199	613
2513	699
3208	877
3323	923
3851	1076
3881	1066
4800	1334
5571	1533
6764	1814

TABLE E2

D_{df} and D_s Data for Reference Spreadfactor Curves
(Stains Created in March 1989)

D_s (μm)	D_{df} (μm)	Polymer Conc. (g/dl)
6054	1703	4.0
5196	1469	4.0
5982	1732	4.0
9594	2767	4.0
8046	2288	4.0
9753	2751	4.0
4970	1431	4.0
4607	1299	4.0
5491	1510	4.0
1708	463	4.0
1372	368	4.0
1680	440	4.0
1490	384	4.0
814	210	4.0
1117	310	4.0
1276	331	4.0
1051	277	4.0
874	240	4.0
762	204	4.0
1138	296	4.0
1258	305	4.0
2815	764	4.0
3572	989	4.0
3697	1039	4.0
4002	1108	4.0
4111	1167	4.0
4562	1288	4.0
2313	699	5.7
2513	809	5.7
2954	1039	5.7
3743	1227	5.7
4340	1395	5.7
4903	1650	5.7
6150	2034	5.7
7030	2459	5.7

9729	3200	5.7
1268	468	7.6
1540	564	7.6
2344	901	7.6
2476	931	7.6
2559	961	7.6
2680	1046	7.6
2882	1104	7.6
3526	1299	7.6
3632	1446	7.6
4436	1716	7.6
4923	1902	7.6

Appendix E